



Research papers

The role of vegetation, soils, and precipitation on water storage and hydrological services in Andean Páramo catchments



Patricio X. Lazo^a, Giovanni M. Mosquera^{a,b,*}, Jeffrey J. McDonnell^c, Patricio Crespo^a

^a Departamento de Recursos Hídricos y Ciencias Ambientales, Facultad de Ingeniería & Facultad de Ciencias Agropecuarias, Universidad de Cuenca, Av. 12 de Abril, Cuenca, Ecuador

^b Institute for Landscape Ecology and Resources Management (ILR), Research Centre for BioSystems, Land Use and Nutrition (IFZ), Justus Liebig University, Giessen, Germany

^c Global Institute for Water Security, University of Saskatchewan, Saskatoon, Canada

ARTICLE INFO

This manuscript was handled by Marco Borga, Editor-in-Chief, with the assistance of Michael Bruen, Associate Editor

Keywords:

Andean Páramo wetlands
Passive storage
Dynamic storage
Peatland
Water regulation
Ecosystem services

ABSTRACT

Understanding how tropical montane catchments store and release water, and the resulting water ecosystem services they provide is crucial for improving water resource management. But while research in high-elevation tropical environments has made progress in defining streamflow generation processes, we still lack fundamental knowledge regarding water storage characteristics of catchments. Here we explore catchment storage and the factors controlling its spatial variability in seven Páramo catchments (0.20–7.53 km²) in southern Ecuador. We applied a field-based approach using hydrometeorological, water stable isotopic, and soils hydrophysical data from a 3 year collection period to estimate the passive (*PasS*) and dynamic (*DynS*) storage of the catchments. We also investigated relations between these storages and landscape and hydrometric variables using linear regression analysis. *PasS* estimates from hydrophysical soil properties and soil water mean transit times were consistent with estimates using streamflow mean transit times. Computed catchment *PasS* and *DynS* for the seven watersheds were 313–617 mm and 29–35 mm, respectively. *PasS* increased directly with the areal proportion of Histosol soils and cushion plant vegetation (wetlands). *DynS* increased linearly with precipitation intensity. Importantly, only 6–10% of the mixing storage of the catchments (*DynS/PasS*) was hydrologically active in their water balance. Wetlands internal to the catchments were important for *PasS*, where constant input of low intensity precipitation sustained wetlands recharge, and thus, the water regulation capacity (i.e., year-round water supply) of Páramo catchments. Our findings provide new insights into the factors controlling the water regulation capacity of Páramo catchments and other peaty soils dominated environments.

1. Introduction

Mountainous headwaters provide key water-related services for downstream ecosystems and populations worldwide (Viviroli et al., 2007). This is particularly true for headwater tropical ecosystems (Aparecido et al., 2018; Asbjornsen et al., 2017; Hamel et al., 2017), such as the Andean Páramo, which occupies over 30,000 km² of northern South America (Hofstede et al., 2003; Wright et al., 2017) and sustains the economy of millions of people in the region (IUCN, 2002). Among the variety of ecosystem services provided by the Páramo, its high water production and regulation (i.e., sustained streamflow production during a water year) capacity are two of the most important (Buytaert, 2004; Poulenard et al., 2003). While recent Páramo hydrology research has focused on the investigation of the factors

controlling the water production capacity of this ecosystem (e.g., Roa-García and Weiler, 2010; Buytaert and Beven, 2011; Crespo et al., 2011, 2012, Mosquera et al., 2015, 2016a, 2016b; Correa et al., 2017; Polk et al., 2017), the factors controlling its water regulation capacity have not been yet studied in detail.

Water regulation by headwater catchments is highly influenced by their capacity to store and release water (Mcnamara et al., 2011). As such, in the last decade, there has been an increasing interest within the hydrological science community towards improving our understanding of catchment water storage (hereafter referred to as ‘catchment storage’). For instance, the study of catchment storage has helped improve our general understanding of the streamflow–storage relationships (e.g., Spence, 2007; Soulsby and Tetzlaff, 2008; Kirchner, 2009; Soulsby et al., 2011; Tetzlaff et al., 2014) and how storage regulation and

* Corresponding author at: Departamento de Recursos Hídricos y Ciencias Ambientales, Facultad de Ingeniería & Facultad de Ciencias Agropecuarias, Universidad de Cuenca, Av. 12 de Abril, Cuenca, Ecuador.

E-mail addresses: Giovanny.mosqueras@ucuenca.edu.ec, giovamosquera@gmail.com (G.M. Mosquera).

<https://doi.org/10.1016/j.jhydrol.2019.03.050>

Received 26 October 2018; Received in revised form 5 March 2019; Accepted 6 March 2019

Available online 16 March 2019

0022-1694/ © 2019 Elsevier B.V. All rights reserved.

Nomenclature			
<i>DynS</i>	Dynamic storage	<i>PasS_(HP)</i>	<i>PasS</i> estimated from the soils' hydrophysical properties
<i>DynS_(ES)</i>	Event scale <i>DynS</i>	<i>PasS_(Q)</i>	<i>PasS</i> estimated from the streamflow MTT
<i>DynS_(LT)</i>	Long-term <i>DynS</i>	<i>PasS_(S)</i>	<i>PasS</i> estimated from the soils' MTT
<i>ET_a</i>	Actual evapotranspiration	<i>Q</i>	Discharge/streamflow
<i>ET_{a(cum)}</i>	Cumulative <i>ET_a</i>	<i>Q_(cum)</i>	Cumulative <i>Q</i>
<i>ET_o</i>	Reference evapotranspiration	<i>Q_f</i>	Normalized fractional <i>Q</i>
<i>f</i>	conversion factor from <i>ET_o</i> to <i>ET_a</i>	<i>S(t)</i>	Water balance based storage volume at time <i>t</i>
<i>i</i>	Mean annual discharge	<i>S_f</i>	Normalized fractional storage
MTT	Mean transit time	TB	Tracer based
<i>P</i>	Precipitation	TTD	Transit time distribution
<i>P_(cum)</i>	Cumulative <i>P</i>	WBB	Water balance based
<i>PasS</i>	Passive storage	ZEO	Zhurucay Ecohydrological observatory
		θ	Soil moisture content

storage–discharge hysteresis depends on the antecedent wetness, flow rates, and catchment scale (Davies and Beven, 2015). These findings in turn, have been extremely useful as basis for the enhancement of the structure of hydrological models (e.g., Sayama and McDonnell, 2009; Nipgen et al., 2015; Soulsby et al., 2015; Birkel and Soulsby, 2016).

Notwithstanding, direct quantification of catchment storage remains difficult because of its largely unobservable nature (Hale et al., 2016) and the marked internal (i.e., subsurface) spatial heterogeneity within and among catchments (Seyfried et al., 2009; Soulsby et al., 2008). In response to this, different approaches such as gravimetric techniques (Hasan et al., 2008; Rosenberg et al., 2012), cosmic ray soil moisture observations (Heidbüchel et al., 2015), soil moisture measurements (Grant et al., 2004; Seyfried et al., 2009), streamflow recession analysis (Birkel et al., 2011; Kirchner, 2009), water balance based (WBB), and tracer-based (TB) techniques (e.g., stable isotopes) (Birkel et al., 2011; Hale et al., 2016; Mcnamara et al., 2011) have been applied in order to investigate these important feature of the hydrologic cycle. Among these, the combination of techniques has proven to provide the most valuable insights into water storage in catchments (Staudinger et al., 2017). The combination of WBB and TB methods, for example, has allowed for an indirect quantification of dynamic storage (storage that is determined by the fluxes of water into and out of the

catchment over a given period of time; Sayama et al., 2011; hereafter referred as *DynS*) and passive storage (the subsurface volume of water stored within the catchment that mixes with incoming precipitation; Dunn et al., 2010; Birkel et al., 2011; hereafter referred as *PasS*). However, to date, only few studies have investigated storage combining different techniques (e.g., Pfister et al., 2017; Staudinger et al., 2017). Few studies too have yet quantified the relation between catchment storage and catchment features (e.g., rainfall temporal variability, vegetation, soils, geology) and this remains an open question in hydrological science (Mcnamara et al., 2011).

Most studies of catchment storage dynamics to date have been conducted in single catchments and using only one of the aforementioned storage quantification methods. The few comparative studies have shown that soils and soil drainability play an important role on catchment storage on Scottish peatland dominated catchments (Tetzlaff et al., 2014) and Canadian boreal wetland dominated catchments (Spence et al., 2011). In contrast, geology and topography have been observed to control storage dynamics in steep forested catchments with well-drained soils in Oregon, USA (Hale et al., 2016; McGuire et al., 2005). Bedrock geology has also been found to control catchment storage dynamics in 16 catchments in Luxembourg (Pfister et al., 2017); whereas catchment elevation controlled storage in 21 Alpine Swiss

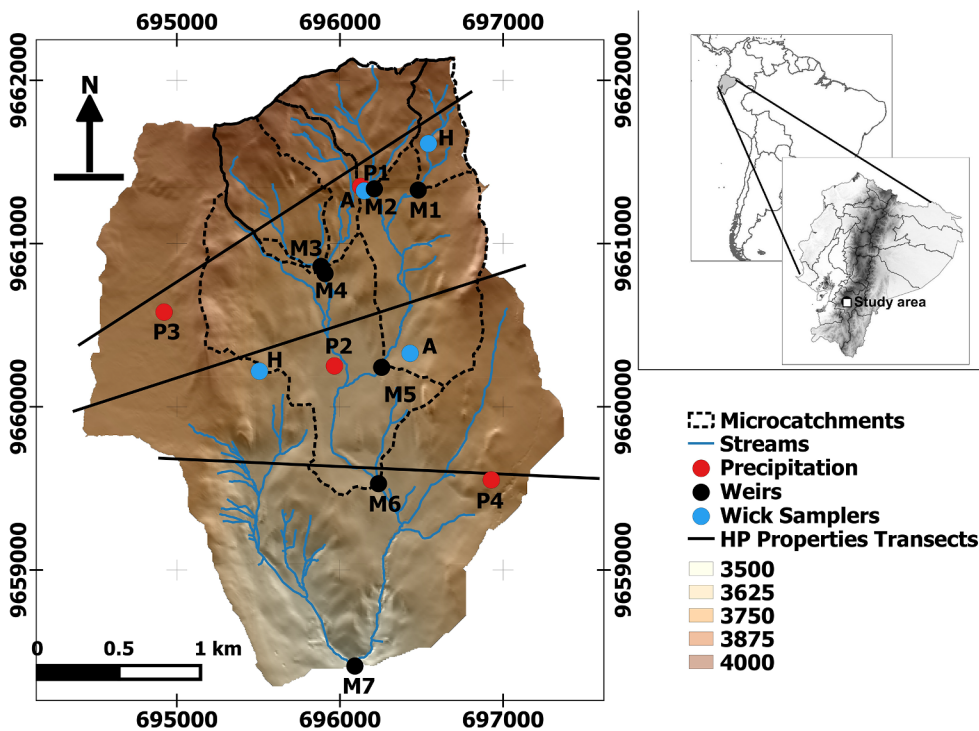


Fig. 1. Location of the study area and the hydrometric and isotopic monitoring network within the Zhurucay Ecohydrological Observatory for: Streamflow (M), Precipitation (P), Andosol (A), and Histosol (H) soils. The solid black lines shown in the figure represent the transects used to characterize the soils' hydrophysical (HP) properties every 150 m within the catchment. *Only rainfall amount data were collected at stations P3 and P4.

catchments as linked to snow versus soil water storage (Staudinger et al., 2017).

Despite these recent efforts aimed at understanding storage and the factors controlling its dynamics in several parts of the world, still there exist many remote and understudied regions (such as the humid tropics) where detailed WBB and TB information are usually lacking. Here we take advantage of a unique dataset of hydrometeorological and isotopic information collected in the nested system of headwater Andean Páramo catchments of the Zhuruca Ecohydrological Observatory (Mosquera et al., 2016a, 2016b; Mosquera et al., 2015). We present new WBB and TB storage estimations using these data, in combination with detailed information on the biophysical features of the landscape (e.g., soil type, vegetation cover, geology, topography, rainfall temporal variability) and soils' hydrophysical properties of the monitored catchments. Our overarching question for this work is: how do vegetation, soils, and precipitation dynamics control passive and dynamic storage across catchments? Our specific research goals are: 1) to compare different PasS calculation methods in order to validate the TB PasS estimations; 2) to quantify the PasS and DynS of the catchments at different temporal scales (event-based to few years); and 3) to examine whether catchment features, if any, control their PasS and DynS. Information that is urgently needed to improve the understanding of the factors that control the water-related ecosystem services (i.e., water production and regulation) provided by the Páramo and the management of water resources of peat-dominated catchments in tropical regions and elsewhere.

2. Materials and methods

2.1. Study site

The study site is the Zhuruca Ecohydrological Observatory (ZEO), located in south Ecuador. The ZEO is situated on the western slope of the Pacific–Atlantic continental divide within the Andean Mountain range. The observatory expands over an altitudinal range between 3400 and 3900 m a.s.l. (Fig. 1). The climate is influenced by both, Atlantic and Pacific regime (Crespo et al., 2011). Mean annual precipitation is 1345 mm with minimal seasonality. Rainfall is composed mainly of drizzle year-round (Padrón et al., 2015). Mean annual temperature is 6.0 °C and mean annual relative humidity is 90% at 3780 m a.s.l. within the study site (Córdova et al., 2015).

The geomorphology is dominated by glaciated U-shape valleys with an average slope of 17%. Most of the land surface (69%) has slopes

below 20%; 5% of the catchment has slopes > 40% (Table 1; Mosquera et al., 2015). The geology of the observatory is composed of mostly volcanic rocks compacted by glacial activity (Coltorti and Ollier, 2000). Two geologic formations dominate the site: (1) The late Miocene Quimsacochoa formation is composed of basaltic flows with plagioclases, feldspars, and andesitic pyroclastics and (2) the Turi formation composed of tuffaceous andesitic breccias, conglomerates, and horizontal stratified sands.

The soils in the study area are mainly Andosols and Histosols (IUSS Working Group WRB, 2015). These soils were formed by the accumulation of volcanic ash over the valley bottoms and low gradient slopes. As a result of the cold, humid environmental conditions, they are black, humic, and acid soils, rich in organic matter with high water storage capacity (Quichimbo et al., 2012). Andosols cover 76% of the observatory and are mainly found on the hillslopes; while the Histosols cover the remaining 24% and are found mainly in flat areas at valley bottoms and toe slope position (Mosquera et al., 2015). Vegetation at the study site is composed by Cushion plants (*Plantago rigida*, *Xenophyllum humile*, *Azorella* spp.), mosses, and lichens mainly covering the Histosols. Tussock grass (*Calamagrostis* sp.) covers the Andosols. In the ZEO, as in most undisturbed Páramo areas, the areal proportion of Histosol soils and cushion plants is strongly correlated ($R^2 = 0.74$, $p = 0.01$) and have led to the formation of “Andean wetlands” (Mosquera et al., 2016a), and hereafter we refer to them simply as wetlands.

2.2. Hydrometric information

Discharge, precipitation amount, and meteorological variables were recorded continuously from November 2011 to November 2014. Discharge was measured in seven nested catchments. It was measured using V-notch weirs in catchments M1–M6 and a rectangular weir at the largest/outlet catchment (M7, Fig. 1). The weirs were instrumented with Schlumberger pressure transducers with a precision of ± 5 mm. Water levels were recorded at a 5-minute resolution and transformed into discharge using the Kindsvater–Shen relationship (U.S. Bureau of Reclamation, 2001). Discharge equations were calibrated using constant rate salt dissolution measurements (following Moore, 2004). Even though the use of a single rain gauge for monitoring precipitation amounts is common in headwater catchments (e.g., Buttle, 2016; Cowie et al., 2017; Pearce et al., 1986; Safeeq and Hunsaker, 2016; Sidle et al., 1995), we used 4 HOBO tipping bucket rain gauges with a resolution of 0.2 mm to capture the spatial variability of precipitation within the ZEO

Table 1
Landscape features and hydrometric variables of the nested system of catchments of the ZEO (From Mosquera et al., 2015).

Catchment	Area (km ²)	Slope (%)	Distribution of soil types (%)		Vegetation Cover (%)				Geology (%)		
			Andosol	Histosol	Tussock grass	Cushion plants	Polylepis Forest	Pine Forest	Turi	Quaternary Deposits	Quimsacochoa
M1	0.20	14	87	13	85	15	0	0	0	0	100
M2	0.38	24	85	15	87	13	0	0	1	33	66
M3	0.38	19	84	16	78	18	4	0	41	0	59
M4	0.65	18	80	20	79	18	3	0	48	1	50
M5	1.40	20	80	20	78	17	0	4	1	30	70
M6	3.28	18	78	22	73	24	1	2	30	20	50
M7	7.53	17	76	24	72	24	2	2	31	13	56

Catchment	Precipitation (mm y ⁻¹)	Total Runoff (mm y ⁻¹)	Runoff Coefficient	Flow rates, as frequency of non-exceedance (l s ⁻¹ km ⁻²)						
				Qmin	Q10	Q30	Q50	Q70	Q90	Qmax
M1	1300	729	0.56	0.7	2.7	6.6	14.3	26.4	50.1	1039.0
M2	1300	720	0.55	1.2	4.8	7.9	14.9	26.7	49.0	762.9
M3	1293	841	0.65	2.3	7.3	10.8	17.7	28.1	52.4	894.2
M4	1294	809	0.62	4.2	6.2	9.8	16.6	27.3	52.1	741.2
M5	1267	766	0.60	1.5	4.1	8.3	15.3	26.9	50.8	905.7
M6	1254	786	0.63	1.2	3.7	8.2	15.9	27.5	53.2	930.4
M7	1277	864	0.68	1.9	4.0	8.7	15.2	29.2	60.8	777.9

(Sucozhañay and Céleri, 2018; Fig. 1). We selected these rain gauges since they have shown to provide optimal spatial distribution of precipitation within the Zhurucay Observatory with no bias and low mean daily precipitation errors ($< \pm 0.25$ mm) in comparison to the use of a dense network of rain gauges ($n = 13$; Seminario, 2016). We used the Kruskal-Wallis test at a statistical significance level of 0.05 to evaluate differences among the 3-years rainfall data recorded by the 4 rain gauges used in this study. Results from the test showed no significant differences (p -value > 0.05) among the rainfall data, as has been previously reported in nearby Páramo areas (Buytaert et al., 2006), we applied the Thiessen polygon method to these data to estimate precipitation at each of our seven monitored catchments.

Meteorological variables were also recorded using a Campbell Scientific meteorological station co-located with the tipping bucket P1 (Fig. 1). Air temperature and relative humidity were recorded with a CS-215 probe protected with a radiation shield. Wind speed was recorded using a Met-One 034B Windset anemometer and solar radiation was recorded with a CS300 Apogee pyranometer. We estimated reference evapotranspiration (ET_o) for each of our study catchments using the FAO-56 Penman-Monteith equation (Allen et al., 1998). For this purpose, we used the near-surface air temperature lapse rate determined by Córdova et al. (2016) in a nearby Páramo area to correct for differences in air temperature with elevation at each of our catchments. No corrections for wind speed, relative humidity, and solar radiation were carried out considering the size of the study area (< 10 km²) and that these environmental variables have shown only limited influence on ET_o estimations within the study area (Córdova et al., 2015).

2.3. Characterization of the soils' hydrophysical properties

Given that the sampling of soils in the study area is labor intensive due to the harsh environmental conditions, we selected three transects (Fig. 1) to collect soil samples for soil properties analyses. Since the physiographic position along the landscape, i.e., valley bottom, toe slope, lower slope, middle slope, upper slope, and hilltop (following FAO, 2009; Schoeneberger et al., 2012), has shown to influence the spatial variability of soil properties in the Páramo (Guio Blanco et al., 2018); the transects were selected to capture this variability among physiographic positions within the catchment. Soil samples were collected at 45 sampling locations (in total) almost equally distributed every 150 m along the selected transects to capture the variability of the soil properties at different physiographic positions. At each sampling location, we characterized the soil depth, soil types, soil horizons (organic and mineral), and the thickness of each horizon. As the presence of Andosol and Histosol soils dominates in our study area, we used the criteria of the IUSS Working Group WRB (2015) to classify their horizons' types. For both soil types, the organic horizon corresponded to soils with organic matter contents higher than 5% and bulk densities lower than 0.90 g cm⁻³, whereas the mineral horizon presented organic matter contents lower than 5% and bulk densities higher than 0.9 g cm⁻³.

Additionally, we collected three undisturbed soil samples of 100 cm³ using steel rings (5 cm diameter) at each sampling location and soil horizon. Following collection, the samples were saturated via capillary rise from a saturated sand support for analysis of the soil water tension–water content (θ) relationships at saturation (pF 0) and field capacity (pF 2.54) at the Soil Hydrophysics Laboratory of the University of Cuenca. The θ at saturation was obtained via gravimetry after the saturated samples were dried up in an oven at 105 °C for 24 h and at field capacity via the ceramic plates system method (USDA and NRCS, 2004). The θ values are reported as volumetric moisture (cm³ cm⁻³).

2.4. Collection and analysis of isotopic data

Weekly water samples for oxygen-18 (¹⁸O) isotope analysis were

collected for the period May 2012–May 2014. These samples were collected in streamflow, precipitation, and soil water. Grab samples in streamflow were collected at the same stations used for measuring discharge. Given the potential spatial variability of the isotopic composition of rainfall (Fischer et al., 2017), water samples in precipitation were collected using two rain collectors located at 3780 and 3700 m a.s.l. (P1 and P2 in Fig. 1, respectively). Precipitation water samples were collected using circular funnels connected to polypropylene rain collectors covered with aluminum foil and with a 5 mm mineral oil layer to reduce evaporation of the stored water (IAEA, 1997). Once precipitation samples were collected, the rain collectors were cleaned, dried, and the mineral oil replaced before their re-installation.

Soil water samples were collected using wick samplers installed at four locations (2 Histosols and 2 Andosols) (Fig. 1). The wick samplers were built with 9.5 mm-diameter fiberglass wicks connected to a polypropylene container of 30 × 30 cm (following Boll et al., 1991, 1992; Knutson et al., 1993). One end of the wick was connected to the wick sampler and the other to a 1.5 L glass bottle where the soil water was collected and stored. In order to collect the mobile soil water fraction (Landon et al., 1999), we applied 1 m length of suction (Holder et al., 1989). The wick samplers were installed at three depths at all soil water sampling stations. In the Histosols, they were placed at 25 and 45 cm depths in the organic horizon and at 75 cm depth in the organic–mineral horizons interface. In the Andosols, they were placed at 25 and 35 cm depths in the organic horizon and at 65 cm depth in the shallowest part of the mineral horizon. The wick samplers in the Histosols were located in flat zones at the valley bottoms near the streams, whereas in the Andosols they were located at the middle and bottom parts of a hillslope. Rainfall and soil water samples were filtered using 0.45 μm filters in order to minimize organic matter contamination. The collected water samples were stored in 2 ml amber glass bottles, covered with parafilm, and kept away from sunlight to minimize any fractionation by evaporation.

A cavity ring-down spectrometer (Picarro L1102-i) was used to measure the $\delta^{18}\text{O}$ isotopic composition of the water samples with a 0.1‰ precision. To diminish the memory effect in the analyses (Penna et al., 2012) and considering that this effect increases when samples from different water types (e.g., precipitation, streamflow, soil water, groundwater) are analyzed together in individual runs, we analyzed water samples of the same type in each run to minimize the memory effect. In addition, we applied six sample injections and discarded the first three as recommended by the manufacturer to further reduce this effect. For the last three injections, we calculated the maximum $\delta^{18}\text{O}$ isotopic composition difference and compared it with the analytical precision given by the manufacturer and the standard deviation of the isotopic standards used for the analyses (0.2‰ for oxygen-18). Samples that showed measurement differences larger than this value were re-analyzed. Contamination of the isotopic signal was checked using ChemCorrect 1.2.0 (Picarro, 2010). This evaluation showed that only 3 soil samples (0.5% of the total) were contaminated with organic compounds. Those samples were excluded from the analysis. Isotopic concentrations are presented in the δ notation and expressed in per mill (‰) according to the Vienna Standard Mean Ocean Water (V-SMOW; Craig, 1961).

2.5. Soil water mean transit time (MTT)

Mean transit time is defined as the time it takes for a water molecule to travel subsurface in a hydrologic system (McGuire and McDonnell, 2006). That is, from the time it enters as precipitation or snow to the time it exists at an outlet point (e.g., streamflow, spring, soil wick sampler, or lysimeter). The approach used to estimate soil water MTT was based on the lumped convolution method (Maloszewski and Zuber, 1996), which assumes a steady-state condition of the flow system. Even though the steady-state assumption has been criticized as an unrealistic catchment representation in a variety of environments, the particular

catchment features (i.e., relatively homogeneous soil distribution and compact geology) and low seasonal variation of hydrometeorological conditions at the ZEO, justify this assumption in our study catchment Mosquera et al. (2016b). This method transforms the input tracer signal (precipitation or snowmelt; δ_{in}) into the output tracer signal (stream, soils; δ_{out}):

$$\delta_{out}(t) = \frac{\int_0^\infty g(\tau)w(t-\tau)\delta_{in}(t-\tau)d\tau}{\int_0^\infty g(\tau)w(t-\tau)d\tau} \tag{1}$$

where, τ is the integration variable representing the MTT of the tracer, $(t - \tau)$ is the time lag between the input and output tracer signals, $g(\tau)$ is the transit time distribution (TTD) that describes the tracer's subsurface transport, and $w(t)$ is a recharge mass variation function. The latter was applied to take into account the temporal variability in recharge rates by weighting the input isotopic composition based on precipitation amounts (McGuire and McDonnell, 2006). As precipitation isotopic composition varies as a function of elevation within the study site, the precipitation input signal for each catchment was corrected using the isotopic lapse rate determined for the ZEO. That is, an increase of 0.31‰ in $\delta^{18}O$ per 100 m decrease in elevation (Mosquera et al., 2016a) We used this isotopic lapse rate and the mean elevation of each study catchment to correct the weekly isotopic data obtained from our two rain gauges used to monitor the input isotopic signal in our study catchment (Mosquera et al., 2016b).

We tested five TTDs for the simulations: the exponential model (EM), exponential–piston flow model (EPM), the dispersion model (DM) (Małozewski and Zuber, 1982), the gamma model (GM) (Kirchner et al., 2000), and the two parallel linear reservoir model (TPLR) (Weiler et al., 2003). Similarly to the findings of Mosquera et al. (2016b) during the evaluation of streamflow MTTs at the ZEO, the TTD that best represented the subsurface transport of water through the soils was the EM. Therefore, the soil water MTTs reported below correspond to the estimations based on this TTD.

2.6. Passive storage estimations

We define passive storage as:

$$PasS = MTT * i \tag{2}$$

where: i is the mean annual discharge over the period MTT was estimated for each catchment or soil horizon. We estimated PasS based on the streamflow MTTs (Table 2) of the nested system of catchments reported by Mosquera et al. (2016b) using the same methodology described in the Section 2.5, and hereafter referred as $PasS_{(Q)}$.

We also approximated the $PasS$ at the outlet of the basin (M7) based on two additional methodologies in order to examine how much of the catchments' $PasS_{(Q)}$ is represented by the soils. The first approach was based on the soils' hydrophysical properties (hereafter referred as $PasS_{(HP)}$). Given the high water retention capacity of the Páramo soils and the sustained year-round rainfall at the study site (Padrón et al., 2015), we assumed that their soil moisture content remained high and near saturation conditions throughout the year (Buytaert, 2004). We also assumed that the contribution of the soils to the catchment $PasS$

should be between saturation and field capacity. As such, we used the θ s at pF 0 (saturation) and pF 2.54 (field capacity) to estimate the water storage for each soil horizon at each of the positions where these soils' hydrophysical properties were measured along the landscape as follows:

$$PasS_{HP(j,k)} = \theta_{(j,k)} * d_{(j,k)} \tag{3}$$

where $PasS_{(HP)}$ represents the soil water storage and d the representative depth of the soil horizon j (i.e., organic or mineral) at position k across the landscape (i.e., from valley bottom to hilltop) where soil moisture θ (at saturation or field capacity) was measured. Using this approach and mapping the landscape surface that corresponded to the different positions k , we estimated the water storage in the soils at each of these positions for the whole catchment. For example, for estimating the $PasS_{(HP)}$ of the catchment at the middle of the slope, we mapped the area of the whole catchment corresponding to a slope of 32–40% and with Andosol soil type (as indicated in Table 3). The total catchment $PasS_{(HP)}$ was then calculated as the sum of $PasS_{(HP)}$ at all monitoring positions for both the organic and mineral horizons at saturation and field capacity.

The second approach was based on the soil water MTT estimations (hereafter referred as $PasS_{(S)}$). The average of the volume of water stored in the bottles used for the weekly collection of soil water samples was used to estimate the i (discharge) value in Eq. (2). This volume was converted to discharge by dividing it to the area of the samplers (30 cm × 30 cm). In this way, we estimated the $PasS_{(S)}$ for each soil type at each monitoring depth and position within the landscape. Given that the tracer signal at an outlet point within a catchment accounts for the mixing of all the flow paths above such points (McGuire and McDonnell, 2006), this approach represents directly the storage of all the water draining down towards the outlet point. Consequently, no further integration of different landscape units is needed. This contrasts with the other alternative method where $PasS_{(HP)}$ requires an integration of the water stored at different parts of the landscape.

2.7. Dynamic storage estimation

The WBB volumes of water stored in the catchments were estimated for each day during the study period following Sayama et al. (2011):

$$S(t) = P(t) - Q(t) - ET_a(t) \tag{4}$$

where: $S(t)$, $P(t)$, $Q(t)$ and $ET_a(t)$ are the storage volume, precipitation, streamflow, and actual evapotranspiration at time t , respectively. The long-term $DynS$ (hereafter referred as $DynS_{(L,T)}$) of the nested catchments was then defined as the difference between the maximum (S_{max}) and the minimum (S_{min}) daily storage volumes obtained from Eq. (3) over the period of analysis.

Actual evapotranspiration was estimated as:

$$ET_a = f * ET_o \tag{5}$$

where: ET_o is the potential evapotranspiration, and f is a factor which was calculated as the result of the difference between P and Q divided by ET_o (i.e., $(P-Q)/ET_o$) for each catchment (Staudinger et al., 2017).

Table 2

Streamflow TB Passive ($PasS_{(Q)}$) and long-term Dynamic Storage ($DynS_{(L,T)}$) estimations for the nested system of catchments at the ZEO using data collected in the period Nov 2011–Nov 2014. *Catchments' MTTs estimations were obtained from Mosquera et al., 2016b.

Catchment	Streamflow MTTs* (days)	Passive Storage (mm)	Dynamic Storage (mm)	Dynamic Storage/Passive storage (%)
M1	194 (171–227)	394 (341–453)	34 (31–37)	9
M2	156 (137–186)	313 (270–361)	31 (28–34)	10
M3	264 (232–310)	617 (534–714)	35 (32–38)	6
M4	240 (212–280)	539 (470–621)	33 (31–36)	6
M5	188 (165–219)	400 (346–460)	32 (29–35)	8
M6	188 (164–220)	411 (353–474)	31 (29–34)	8
M7	191 (167–224)	457 (395–530)	29 (26–32)	6

Table 3

Hydrophysical properties for each soil type, horizon, and position within the ZEO and passive storage estimations based on these properties ($PasS_{(HP)}$) in relation to the areal extent of each of them with respect to the total basin area, M7. $PasS_{(HP)}$ estimates were calculated for the soils' moisture contents (θ) at field capacity (FC, pF 2.54) and saturation (Sat, pF 0) conditions. *As a percentage of total catchment area (7.53 km²). **Total $PasS_{(HP)}$ per soil type (Andosol and Histosol soils) and horizon (organic and mineral).

	Hillslope position	Soil type	Slope (%)	Soil thickness (cm)	Area* (%)	Number of samples	θ_{FC} (cm ³ cm ⁻³)	θ_{Sat} (cm ³ cm ⁻³)	$PasS_{(HP)}$		Total**	
									FC (mm)	Sat (mm)	FC (mm)	Sat (mm)
Organic Horizon	Valley bottom	Histosol	1–5	70	0.9	27	0.62	0.90	17	24	441	623
		Histosol	5–15	70	23.1	5	0.63	0.89	424	599		
	Toe slope	Andosol		40	3.5	5	0.62	0.72	11	13	230	264
		Andosol	15–32	30	22.0	5	0.67	0.83	58	72		
	Lower slope	Andosol	32–40	35	33.3	10	0.69	0.76	106	117		
	Middle slope	Andosol	40–56	38	7.8	5	0.65	0.74	25	29		
		Andosol	> 56	38	5.6	4	0.65	0.74	18	21		
	Upper slope	Andosol	1–5	34	3.7	7	0.65	0.73	11	12		
		Andosol										
	Mineral Horizon	Valley bottom	Histosol	1–5	50	0.9	27	0.54	0.65	10	13	270
Histosol			5–15	50	23.1	5	0.54	0.65	260	312		
Toe slope		Andosol		30	3.5	5	0.50	0.53	7	7	131	156
		Andosol	15–32	30	22.0	5	0.46	0.56	40	49		
Lower slope		Andosol	32–40	30	33.3	10	0.46	0.56	61	74		
Middle slope		Andosol	40–56	20	7.8	5	0.46	0.53	9	11		
		Andosol	> 56	20	5.6	4	0.46	0.53	7	8		
Upper slope		Andosol	1–5	31	3.7	7	0.46	0.53	7	8		
		Andosol										

2.8. Runoff events selection and variables

We selected rainfall–runoff events for the analysis of the temporal variability of $DynS$ at the event scale (hereafter referred as $DynS_{(ES)}$). These events were defined as runoff response to rainfall inputs where discharge increased from below low flow values (Smakhtin, 2001) – below Q_{35} non-exceedance flow rates (determined as low flows at the ZEO, Mosquera et al., 2015) – to values higher than this threshold during the duration of the events. We further used the minimum inter-event time criteria, defined as the minimum time lapse without precipitation between two consecutive events (Dunkerley, 2008), to separate the precipitation time series into rainfall events. Given that at the study region rainfall occurs frequently and is sustained along the year (Padrón et al., 2015), we selected a minimum inter-event time of 6-hr to define independent events. Although rainfall–runoff events were evaluated at all catchments, only the results for the outlet of the catchment (M7) are reported as similar trends for all catchments were found. Under these considerations, 42 events were selected for the analysis at M7.

For each event, we evaluated the storage–discharge hysteresis. This was conducted by visual inspection of the plots of the normalized fractional storage S_f and fractional discharge Q_f (Davies and Beven, 2015). These values are defined as the storage and discharge volumes as fractions of the $PasS_{(Q)}$ (i.e., $S_f = S/PasS_{(Q)}$ and $Q_f = Q/PasS_{(Q)}$, respectively), where S and Q are the same as in Eq. (3), but estimated at 5-minute temporal resolution for the analysis at the event scale.

Additionally, we also estimated the cumulative Q ($Q_{(cum)}$), cumulative P ($P_{(cum)}$), cumulative ET_a ($ET_{a(cum)}$), the minimum, mean, and maximum rainfall intensity, as well as the antecedent wetness conditions of the catchment represented as the amount of antecedent precipitation over different time periods (7 and 14 days before each event) for each of the 42 events to investigate the influence of these hydro-meteorological variables on $DynS_{(ES)}$.

2.9. Statistical analysis between storage and landscape–hydrometric features

We conducted a Pearson linear correlation analysis between the estimates of $PasS_{(Q)}$ and $DynS_{(LT)}$ and different landscape features which included: catchment area, soil type, vegetation cover, geology, and average slope of each catchment. We also conducted a linear

correlation analysis between $PasS_{(Q)}$ and $DynS_{(LT)}$ with hydrometric variables that included mean annual P , mean annual Q , mean annual ET_a , runoff coefficient (Q/P), and different non-exceedance flow rates according to the catchment's flow duration curves. The biophysical and hydrometric features of the catchments were obtained from Mosquera et al. (2015) (Table 1).

At the event scale, linear correlation analysis was used to investigate relations between $DynS_{(ES)}$ with all the hydrometeorological variables estimated for the rainfall–runoff events (Section 2.8). All correlations were evaluated using the determination coefficient (R^2) at a statistical significance level of 0.10 (i.e., 90% confidence level) using the t-student test.

3. Results

3.1. Catchment water passive storage

3.1.1. Streamflow MTT based catchment passive storage estimations

The $PasS_{(Q)}$ variation among the catchments was relatively large (304 mm). These estimates varied from 313 to 617 mm, with a value of 457 mm at the outlet of the basin (M7). The maximum values were observed at catchments M3 and M4, while the minimum value at M2 (Table 2).

3.1.2. Hydrophysical soil properties based catchment passive storage estimations

The hydrophysical properties of the soils (i.e., θ at pFs 0 and 2.54) located at the different landscape positions and their areal extent within the ZEO are presented in Table 3. The Histosols were only found at the valley bottom and toe slope positions. Their average thickness was 70 cm for the organic horizon and 50 cm for the mineral horizon. Histosols were normally found in low relief areas with slopes between 1 and 15%. They presented the highest θ s at saturation (pF 0) for the organic (0.89–0.90 cm³ cm⁻³) and the mineral horizon (0.65 cm³ cm⁻³). The organic horizon of the Histosols had significantly higher θ s at field capacity (pF 2.54; 0.62–0.63 cm³ cm⁻³) in comparison to the mineral horizon (0.54 cm³ cm⁻³). The Andosols on the other hand, were found from the toe slope to the summit positions with slopes between 1 and 56%. Their thickness was more variable than for the Histosols, and ranged between 30 and 40 cm for the organic horizon and 20–30 cm for the mineral horizon. The θ values at saturation of the

organic horizon of the Andosols ($0.72\text{--}0.83\text{ cm}^3\text{ cm}^{-3}$) were more variable than those of their mineral horizon ($0.53\text{--}0.56\text{ cm}^3\text{ cm}^{-3}$). For both horizons, these values were significantly lower than for the Histosols. Their θ values at field capacity for the organic horizon of these soils ($0.62\text{--}0.69\text{ cm}^3\text{ mm}^{-3}$) were more variable and higher than those for their mineral horizons ($0.46\text{--}0.50\text{ cm}^3\text{ cm}^{-3}$).

The $PasS_{(HP)}$ was variable among the different soil types and horizons at the different positions in the landscape (Table 3). The $PasS_{(HP)}$ estimations using these soil properties and the spatial distribution and thickness of each soil horizon showed that the Histosols stored a higher amount of water (711 mm at FC and 948 mm at saturation) than the Andosols (361 mm at FC and 420 mm at saturation) (Table 4). Integrating these $PasS_{(HP)}$ values to the catchment scale using the areal proportions of the catchment covered by each soil type, the $PasS_{(HP)}$ at the outlet of the basin (M7) were 445 mm at field capacity and 547 mm at saturation (Table 4).

3.1.3. Soil water MTT based catchment passive storage estimations

Soil water MTTs for Andosols and Histosols at the three monitored depths are reported in Table 5. The MTTs in both soil types increased with depth. MTTs in the Andosols were 35 and 48 days for the shallower organic horizons and 144 days for the organic–mineral horizons interface. MTTs in the Histosols were longer than in the Andosols, with values of 212 and 292 days for the shallower organic horizons and 338 days for the organic–mineral horizon interface. With these MTT values we estimated the $PasS_{(S)}$ for each soil type at each monitoring depth (Table 5). Andosols showed $PasS_{(S)}$ values ranging between 14 and 49 mm, with the highest contribution from the mineral horizon (at 65 cm depth). Histosols showed higher $PasS_{(S)}$ values. Similar to the soil water MTTs, these values increased with depth. $PasS_{(S)}$ was 191 and 263 mm at the shallower organic horizons and 304 mm at the organic–mineral horizon interface (at 65 cm depth). Based on the $PasS_{(S)}$ values at each soil type and horizon, the water storage was 97 mm for the Andosols and 759 mm for the Histosols.

3.2. Catchment water dynamic storage

3.2.1. Long-term dynamic storage estimations

The catchments $DynS_{(LT)}$ ranged from 29 to 35 mm, showing little differences among subcatchments (6 mm). Similar to the $PasS_{(Q)}$, catchments M3 and M4 showed the maximum values, while the minimum value corresponded to M7. The fractions of $DynS_{(LT)}$ to $PasS_{(Q)}$ varied between 6 and 10% among the catchments (Table 2).

Fig. 2 shows the daily temporal variability of the WBB catchments' water storage volume. The system showed a very flashy response of storage volume to precipitation but normally returned to a condition with $S(t)$ of approximately 0 mm day^{-1} . Negative values ($S(t) < 0\text{ mm day}^{-1}$; when the system loses or discharges higher amounts of water than the inputs) and positive values ($S(t) > 0\text{ mm day}^{-1}$; when the system gains or receives higher amounts of water than it discharges) occurred at approximately the same frequency (53 and 47%, respectively).

3.2.2. Event-based dynamic storage estimations

The 42 rainfall–runoff events selected for the analysis represented a wide variety of hydrometeorologic conditions during the study period. The $P_{(cum)}$ at the end of the events ranged between 0.2 and 56.0 mm; with $Q_{(cum)}$ varying between 1.2 and 52.8 mm, $ET_{a(cum)}$ between 0.1 and 16.6 mm, and $DynS_{(ES)}$ between 0.07 and 1.91 mm. In addition, maximum, mean, and minimum P intensities during the events were in the range of $0.6\text{--}22.3\text{ mm h}^{-1}$, $0.1\text{--}5.4\text{ mm h}^{-1}$, and $0\text{ to }1.1\text{ mm h}^{-1}$, respectively. Antecedent P for 7 and 14 days prior to the start of the events ranged between 2.6 and 68.5 mm and 15.8–113.3 mm.

The temporal variability of S_f during the events was similar for all catchments. A representative storm for the catchment (M7) outlet is shown in Fig. 3. The event had a total duration of 50 h and during this

period $P_{(cum)}$ and $Q_{(cum)}$ were 32.2 and 32.3 mm, respectively. Fig. 3 shows that at the beginning of the event (t_0), the system was neither storing nor releasing water (with $S_f = 0$). During the first 17.7 h (t_1) of the event, 82% of the $P_{(cum)}$ entered to the system. During this hydrograph rising limb (black line in Fig. 3a), the catchment both released water via Q in response to the P inputs but was also dynamically recharged ($S_f > 0\text{ mm}$). Thereafter, and once rainfall intensity decreased, the system continued to change from a diminished recharge state to a releasing water state until t_2 at around 18.3 hr. This period of water loss from the catchment was mostly linear. The hydrograph peak (t_2) was mostly caused by contribution of the moisture from the recharged system rather than from precipitation inputs directly (i.e. the black line in the negative region of the S_f during the $t_1\text{--}t_2$ period in Fig. 3b). After rainfall cessation, the release of water from the catchment continued until t_3 (18.6 h). At this point, the hydrograph recession decreased linearly until the end of the event, when the system again reached a stability condition ($S_f \approx 0\text{ mm}$) at 50 h (t_f). The S_f dynamics at the event scale formed an anticlockwise hysteretic loop. All of the monitored events at all catchments followed the same hysteretic direction.

3.3. Relations between storage metrics and landscape features and hydrometric variables

The $PasS_{(Q)}$ for our nested catchments was significantly positively correlated with mean annual Q ($R^2 = 0.73$, $p = 0.07$), runoff coefficient ($R^2 = 0.75$, $p = 0.06$), and high flows represented by the Q_{90} non-exceedance flows ($R^2 = 0.67$, $p = 0.09$) (Table 6). $PasS_{(Q)}$ was also significantly positively correlated with the cushion plants vegetation cover ($R^2 = 0.68$, $p = 0.08$) and negatively correlated with the tussock grass vegetation cover ($R^2 = 0.73$, $p = 0.07$) (Fig. 4). Even though similar correlation trends were found between the catchments' $PasS_{(Q)}$ and their soils' areal extent (i.e., positive for the Histosols and negative for the Andosols), these correlations were not statistically significant ($R^2 < 0.55$, $p > 0.15$). The latter was most likely as a result of the higher uncertainty in the soil type distribution mapping of the ZEO in relation to the vegetation distribution mapping that was better characterized directly in the field (Mosquera et al., 2015).

For the $DynS_{(LT)}$ estimations calculated from the daily WBB analysis, we found statistically significant correlations with landscape and hydrologic variables. However, due to the small range of variation of $DynS_{(LT)}$ among catchments (only 6 mm, Table 2), we acknowledge that these correlations may not be causal and thus do not report them. On the short term, when analyzing correlation between hydrometeorological variables and the $DynS_{(ES)}$ during the events monitored at the outlet of the basin, M7, we identified non-significant correlations between this storage metric and most hydrometeorological variables ($R^2 \leq 0.30$, $p > 0.10$). These variables included the $P_{(cum)}$, $Q_{(cum)}$, $ET_{a(cum)}$, mean and minimum P intensities, and 7 and 14 days accumulated antecedent P. The only significant correlation found was

Table 4

Passive storage estimations based on the soils' hydrophysical properties ($PasS_{(HP)}$) at field capacity (FC) and saturation (Sat) for the organic and mineral horizon of the Andosols and Histosols (Table 3) and the integration of these storages to the catchment outlet, M7, based on the areal extent of each soil type within the ZEO. *Total $PasS_{(HP)}$ = Organic horizon $PasS_{(HP)}$ + Mineral horizon $PasS_{(HP)}$.

	FC (mm)		Sat (mm)	
	Histosol	Andosol	Histosol	Andosol
Organic horizon	441	230	623	264
Mineral horizon	270	131	325	156
Total $PasS_{(HP)}$	711	361	948	420
Soil type percentage (%)	24	76	24	76
Catchment $PasS_{(HP)}$	445		547	

Table 5

Soil water discharge (i), soil water MTTs, and soil water TB passive storage ($PasS_{(S)}$) for the monitored soil types and depths using data collected in the period Nov 2011–Nov 2014. Values in parenthesis correspond to the 5% and 95% confidence intervals.

Soils	i (mm/day)	MTT (days)	$PasS_{(S)}$ (mm)
Andosol–25	0.95	35 (26–48)	33 (25–45)
Andosol–35	0.30	48 (39–59)	14 (11–17)
Andosol–65	0.34	144 (119–166)	49 (41–57)
Histosol–25	0.90	212 (187–247)	191 (168–222)
Histosol–45	0.90	292 (263–331)	263 (236–298)
Histosol–70	0.90	338 (298–394)	304 (268–355)

between the $DynS_{(ES)}$ and the maximum P intensity during the events ($R^2 = 0.91$, $p < 0.001$, Fig. 5).

4. Discussion

Hydrologic services provided by natural ecosystems help improve the well-being of surrounding and downstream societies (Brauman et al., 2007). However, there is still an important knowledge gap regarding the relation between the (eco)hydrological behavior of catchments (e.g., water storage and release) and the hydrologic services (e.g., water production and regulation) that they provide (Sun et al., 2017). Our work presented here on how catchment storage influences the Páramo water regulation capacity shows how highly organic and porous peaty Páramo soils (Histosols) and the local environmental conditions (high humidity and year-round low intensity precipitation) interact to control the water regulation capacity of the ecosystem. Below we discuss key findings and contextualize our work with other sites where peaty soils dominate in the tropics and elsewhere.

4.1. Passive water storage at the catchment scale

4.1.1. Comparison of passive storage estimation methods

Regarding the application of different methods for estimating the catchments' $PasS$ capacity, past investigations have yielded differing results (e.g., Brauer et al., 2013; Staudinger et al., 2017). For instance, at the Girnock catchment in the Scottish highlands, several methods used to estimate the catchment's $PasS$ yielded different results. These methods included the streamflow MTT based ($PasS_{(Q)}$) (Soulsby et al., 2009), a combination of distributed soil moisture and groundwater measurements and hydrologic modelling (van Huijgevoort et al., 2016),

bedrock geophysical surveys (Tetzlaff et al., 2015a), and tracer-based hydrologic modelling (Birkel et al., 2011), with the estimated $PasS$ values yielded amongst these methods varying within two orders of magnitude. For this reason, we first evaluated how our streamflow MTT based passive storage $PasS_{(Q)}$ estimations compared to those based on the monitoring of the soils' hydrophysical properties ($PasS_{(HP)}$) and soil water MTTs ($PasS_{(S)}$).

The $PasS_{(HP)}$ estimates for the catchment outlet (M7) at field capacity and saturation (445 and 547 mm, respectively, Table 4) showed a remarkable agreement with respect to the $PasS_{(Q)}$ estimate (457 mm, Table 2). For $PasS$ estimations based on the soil water MTTs ($PasS_{(S)}$), landscape configuration affected the isotopic signal whereby the water from the Andosols draining down the hillslopes was already mixed at the valley bottom wetlands (Mosquera et al., 2016a; Tetzlaff et al., 2014). As a result, the storage estimations from the Histosols added to the Andosols storage. The sum of the $PasS_{(S)}$ estimations of the organic horizons of the Histosols (i.e., at 25 and 45 cm depth) resulted in a total $PasS$ of 454 mm (Table 5). This values was also very similar to the $PasS_{(Q)}$ estimation. These findings suggest that $PasS_{(Q)}$ provides accurate estimates of the total catchment $PasS$ and that catchment water storage capacity of the ZEO outlet is effectively stored in the Páramo soils. Consequently, deep groundwater sources to runoff are minimal, as has been hypothesized in past studies at the ZEO (Correa et al., 2017; Mosquera et al., 2016a,b). These findings also suggest that the tracer signals from different parts of the catchments become well mixed within the valley bottom wetlands (Mosquera et al., 2016b) and that the integration of these signals provides accurate estimates of catchment passive storage.

Streamflow based MTT has been used to estimate passive storage ($PasS_{(Q)}$) in past investigations (e.g., Soulsby et al., 2009; Mcnamara et al., 2011; Tetzlaff et al., 2015b; Hale et al., 2016; Staudinger et al., 2017). But the accuracy of this method has been difficult to evaluate due the unobservable nature of large groundwater contributions to $PasS$. In these sense, the ZEO hydrologic conditions—where we can exclude a groundwater component—is an ideal site for investigating the accuracy of the $PasS_{(Q)}$ method. Given that the $PasS_{(Q)}$ estimations for the outlet of the catchment lie within those yielded by the potential storage of the soils (i.e., the $PasS_{(HP)}$ estimations at saturation and field capacity), our results show that this method yields accurate catchment $PasS$ estimations.

In other catchments, we hypothesize that through the combined application of both these methods, indirect estimations of groundwater contributions can be obtained. Contributions that are still difficult to quantify in the field or are estimated with high uncertainty using

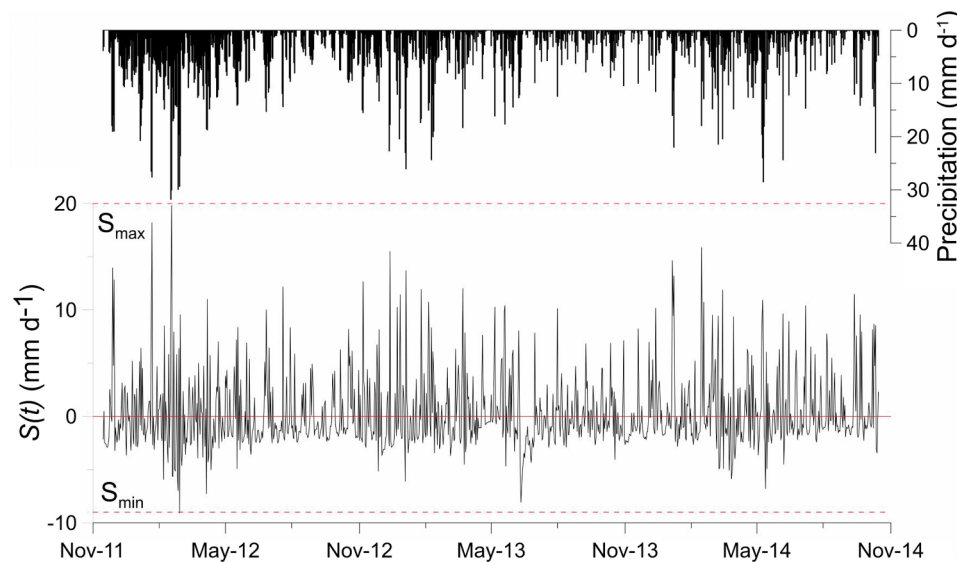


Fig. 2. Daily precipitation and change of storage volume $S(t)$ at the outlet of the catchment (M7) for the period Nov 2011–Nov 2014. The solid red line represents $S = 0 \text{ mm day}^{-1}$ and the dashed red lines represent the maximum (S_{max}) and minimum (S_{min}) storage volumes used to estimate the long-term dynamic storage ($DynS_{(LT)} = S_{max} - S_{min}$). (For interpretation of the references to colour in this figure legend, the reader is referred to the web version of this article.)

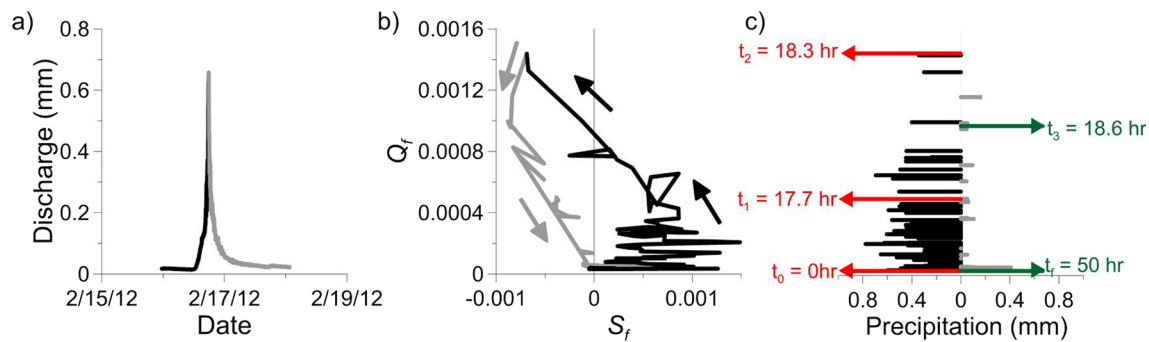


Fig. 3. a) Discharge hydrograph; b) temporal variability of the normalized fractional discharge (Q_f) and storage (S_f) volumes; and c) rainfall amount during a representative rainfall–runoff event at the study site. The data correspond to an event monitored at the outlet of the basin (M7) on February 16th, 2012. The black and grey lines correspond to the rising and recession limbs of the hydrograph, respectively. The red and green lines in subplot c) represent time during the rising and recession limbs of the hydrograph in subplot a), respectively. (For interpretation of the references to colour in this figure legend, the reader is referred to the web version of this article.)

Table 6

Determination coefficients (R^2) between the streamflow TB passive storage ($PasS_{(Q)}$) of the catchments with landscape features and hydrologic variables. Values in bold represent significant correlations at a statistical level of 0.10 (i.e., 90% confidence level). \pm values represents positive or negative correlations between variables, respectively. Q_{xx} represents the flow rates, as frequency of non-exceedance, where xx shows the non-exceedance rate.

Variable name		$PasS_{(Q)}$	
Hydrologic variables	Dynamic Storage (mm)	-0.20	
	Passive Storage	1.00	
	Mean Annual Precipitation	-0.30	
	Mean Annual Discharge	0.73	
	Runoff Coefficient	0.75	
	Q_{min}	0.24	
	Q_{10}	-0.18	
	Q_{30}	0.10	
	Q_{50}	0.13	
	Q_{70}	0.55	
	Q_{90}	0.67	
	Q_{max}	0.03	
	Landscape features	Area (km^2)	0.61
		Slope (%)	-0.45
Andosols (% of total area)		-0.56	
Histosols (% of total area)		0.51	
Tussock Grass (% of total area)		- 0.73	
Cushion plants (% of total area)		0.68	
Turi Formation (% of total area)		0.48	
Quaternary Deposits (% of total area)		-0.28	
Quimsacocha Formation (% of total area)	-0.05		

hydrologic models (e.g., Birkel et al., 2011; Tetzlaff et al., 2014, 2015a; van Huijgevoort et al., 2016). For example, for catchment M3, which is influenced by the additional contribution of water from a shallow spring source to discharge, $PasS_{(HP)}$ estimations ranged between 399 and 472 mm at field capacity and saturation, respectively. The $PasS_{(Q)}$ for this catchment was 617 mm (Table 2). Assuming that the potential water storage capacity of the soils in this catchment were at saturation, it can be assumed that the extra storage capacity provided by this catchment (i.e., the storage added by the additional spring water contribution) is the difference between the $PasS$ estimates yielded by these methods, i.e., about 145 mm. These results suggest the usefulness of both the $PasS_{(Q)}$ and $PasS_{(HP)}$ methods for providing indirect $PasS$ groundwater estimations elsewhere.

4.1.2. Passive storage estimation in relation to other catchments

A summary of the studies in which $PasS$ has been evaluated using different calculation methods in peat-dominated catchments is shown in Table 7. Our estimated $PasS_{(Q)}$ values at the ZEO (313–617 mm, Table 2) are similar to those reported by Bishop et al. (2011) via the

modelling of soil properties at the Gardsjön catchment in Sweden (300 mm) and Soulsby et al. (2009, 2011) using TB methods in a group of montane Scottish catchments (265–688 mm). They attributed these relatively small storage values to the retention of water in the relatively shallow (< 2 m) peat type soils with little deeply sourced water contributions from groundwater storage. By contrast, our estimates are low relative to peat-dominated catchments in North Sweden estimated using soil moisture modelling (1189–1485 mm) by Amvrosiadi et al. (2017). They are also low in relation to the values reported by Birkel et al. (2011) estimated via TB methods and van Huijgevoort et al. (2016) estimated using a TB distributed hydrological model for the peat-dominated Girnock catchment in the Scottish highlands (1000 and 898 mm, respectively). Our values were also lower than those of non-peat-dominated catchments with different land covers (e.g., pasture, grasslands, and forests) in a gradient between the Swiss plateau and alpine regions (> 5000 mm) reported by Staudinger et al. (2017). Despite the differences in catchment features (e.g., precipitation seasonality, land cover, soil type and depth) among the study sites investigated by these authors, they all attributed these high $PasS_{(Q)}$ estimates to water storage in deep groundwater reservoirs. That is, the highly fractured and permeable parental material. At the ZEO, prior research has shown that water stored in the peat type Histosol soils (i.e., wetlands) controls runoff generation (Correa et al., 2016; Mosquera et al., 2015). In addition, other studies have also shown that water originated from these wetlands is the main contributor to runoff year-round and that deeply sourced groundwater contributions to runoff are minimal (Correa et al., 2017; Mosquera et al., 2016a). Our $PasS_{(Q)}$ estimates, similar to those in catchments with low groundwater storage availability and much lower than those in catchments with highly fractured geology, evidence that these wetlands do not only control water production at the ZEO, but also the catchment’s water storage capacity.

4.1.3. How vegetation, soils, and precipitation control passive storage?

Past research at the ZEO has shown the importance of the wetlands (i.e., Histosols and cushion plants vegetation) on the catchments’ water production (Correa et al., 2017, 2016; Mosquera et al., 2015). The high correlation between $PasS_{(Q)}$ and the wetlands cover in our nested system of catchments (Table 6, Fig. 4) suggests that the wetlands also influence the catchments’ available storage for mixing. Similar hydrologic dependence on wetlands storage has been reported at the Scottish Highlands (e.g., Birkel et al., 2011; Tetzlaff et al., 2014; Geris et al., 2015a,b, Geris et al., 2017). These findings also confirm that for catchments with low groundwater contribution, the totality of $PasS_{(Q)}$ depends on their areal proportion of wetlands. Additionally, the strong correlation between $PasS_{(Q)}$ with the catchments’ mean annual discharge and runoff coefficients ($R^2 > 0.73$, Table 6), further evidences

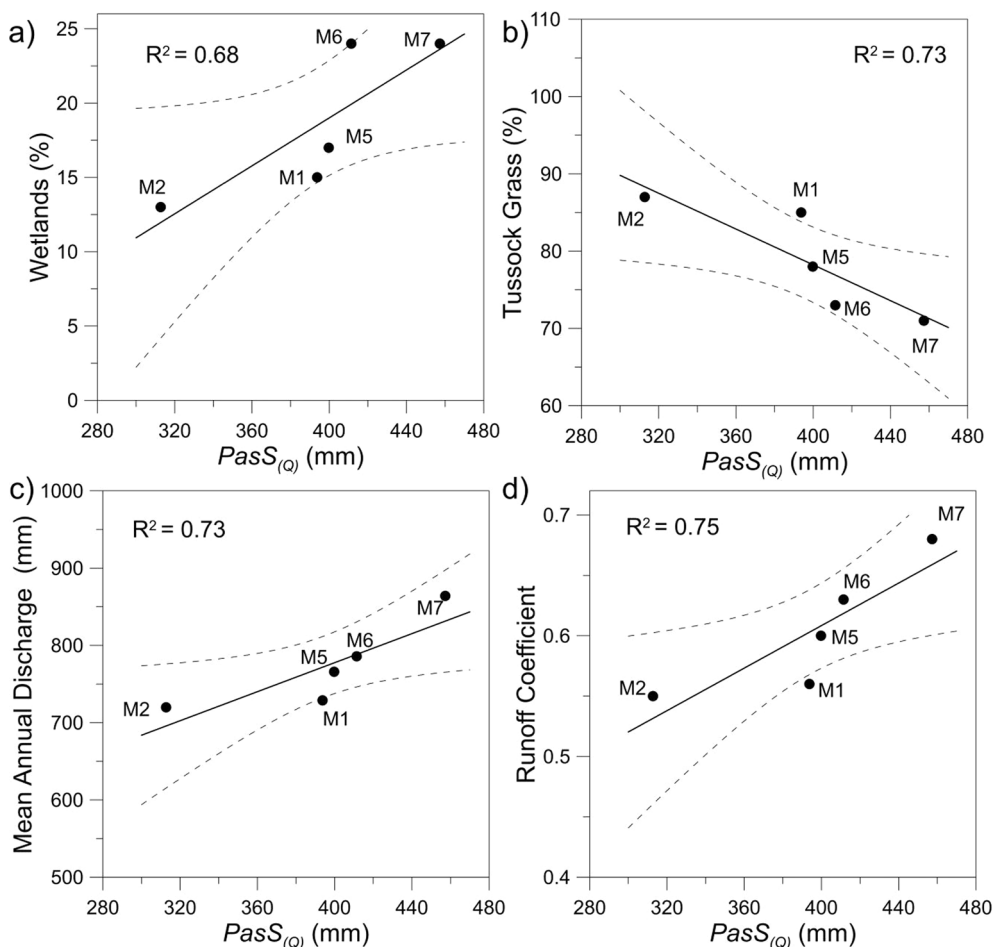


Fig. 4. Relationships between the streamflow TB passive storage ($PasS_{(Q)}$) with a) cushion plants coverage, b) tussock grass coverage, c) mean annual discharge, and d) runoff coefficient of the nested system of catchments. Vegetation is expressed as the percentage of the areal extent of each vegetation type to the total area of each catchment. Dashed lines represent the 5% and 95% confidence intervals of the relationships. Note: Given that water samples used for the estimation of streamflow mean transit times were collected during baseflow conditions (Mosquera et al., 2016b), we excluded data from catchments M3 and M4 in the regression analysis to remove the effect of contributions from a spring water source to these small headwater catchments (Mosquera et al., 2015).

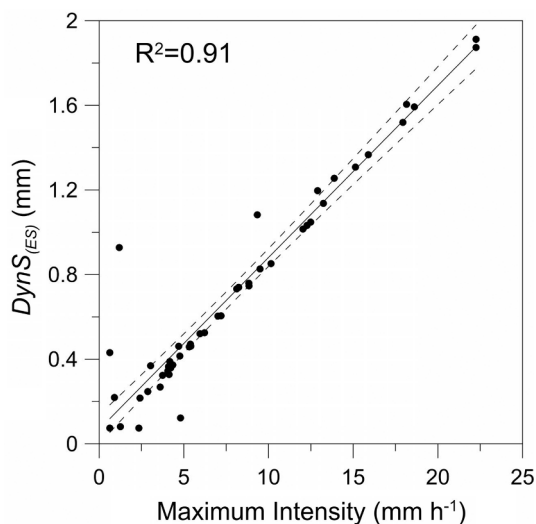


Fig. 5. Relationship between the event scale dynamic storage ($DynS_{(ES)}$) and maximum precipitation intensity during the runoff events ($n = 42$) at the outlet of the basin, M7. Dashed lines represent the 5% and 95% confidence intervals of the relationship.

how the wetlands storage influence runoff generation and regulation. Here, it is worth noting that even though wetlands cover only a relatively small proportion of the monitored catchment areas (i.e., 13–24%, Table 1), they control the catchments’ water production and storage at the ZEO. These findings highlight the importance and the fragility of riparian wetlands as the main – and in this particular case, the only –

water storage reservoir in ecosystems where the presence of peaty soil (i.e., Histosols) dominates.

We also identified some $PasS$ variations among the monitored catchments worth highlighting. For instance, even though two of the smaller headwater catchments M1 (0.20 km²) and M2 (0.38 km²) have similar areal proportions covered by wetlands (13–15%), the smallest catchment M1 showed a much larger $PasS_{(Q)}$ than M2 (394 mm versus 313 mm, respectively). In contrast, even though catchments M5 (1.40 km²) and M6 (3.28 km²) also have similar wetland coverage (20–22%), they presented similar $PasS_{(Q)}$ (400–411 mm). These apparent discrepancies likely result from differences in the catchments’ average slopes as a metric of topography. For example, the steepest topography of catchment M2 (24%) in relation to M1 (14%) is likely to explain the lowest $PasS_{(Q)}$ of catchment M2. On the contrary, catchments M5 and M6 have similar slopes (18–20%, Table 1), factor that seems to explain the similar amount of water stored by these catchments. Similar findings have been reported on Scottish peat-dominated catchments by Tetzlaff et al. (2014). These authors reported that low gradient terrain produced poor drainage conditions, thus, ensuring high volumes of water retained in peaty soils throughout the year whereas steeper terrain that enhances hydraulic gradients allows an enhanced water movement, thus, reducing the amount of water stored in the soils. This combination of factors influencing the catchments’ $PasS$ has also been reported at other sites with different soil types (e.g., Sidle et al., 2001; Lehmann et al., 2007; Detty and McGuire, 2010; Soulsby et al., 2016). Overall, these findings evidence that that even though we did not find a direct relationship between the catchments’ average slopes and their $PasS_{(Q)}$ via correlation analysis, catchments’ topography exerts controls in the amount of water available for internal mixing.

It is also worth noting that two of the upper catchments (M3 and

Table 7
Overview of studies in which $PasS$ has been evaluated in peat-dominated catchments.

Study	Location	Drainage area (km ²)	Altitudinal range (m a.s.l.)	Average slope (%)	Soil type	Method	$PasS$ (mm)
Bishop et al. (2011) Soulsby et al. (2009, 2011)	Gårdsjön Covered Catchment, Sweden Scottish Highlands and Lowlands	6.3 0.5–1800	123–143 > 200	5–50 7–35	Shallow podzol and peats peats, gleys, regosol, and podzols	Soil properties modelling Tracer based (chloride and ¹⁸ O)	300 265–688
Amyrosiadi et al. (2017)	Svarberget catchment, Sweden	2.54	250–260	6.43	Well-developed podzols and peats	Soil moisture modelling	1189–1485
Birkel et al. (2011)	Girnock and Brutland Burn catchments, Scotland	3.6–30.4	250–850	17.5–23	Gley, peat, and podzols	Tracer based (¹⁸ O)	1000
van Huijgevoort et al. (2016)	Brutland Burn catchment, Scotland	3.2	248–538	23	Gley, peat, and podzols	Soil moisture and groundwater hydrologic modelling	898

M4, Fig. 1) showed the highest $PasS_{(Q)}$ (617 and 539 mm, respectively) among all monitored catchments within the ZEO. Also, $PasS_{(Q)}$ of catchment M3 was almost double than that of M2 (Table 2) despite they both have the same catchment areas. Similar findings have been reported by Birkel et al. (2011) and Soulsby et al. (2011) for a group of montane Scottish catchments with similar soil conditions. These authors found that catchments with fractured and permeable geology showed much higher $PasS_{(Q)}$ than catchments with less weathered and more impermeable bedrock. At the ZEO, catchments M3 and M4 showed the longest streamflow MTTs (Mosquera et al., 2016b) and the highest baseflows (Mosquera et al., 2015) among the monitored catchments as a result of a shallow spring water contribution to runoff (i.e., from the weathered mineral horizon or the fractured shallow bedrock) (Correa et al., 2017). Together, these findings suggest that even when the hydrology of the ZEO is dominated by water flowing in the shallow organic horizon of the Páramo soils (Correa et al., 2017; Mosquera et al., 2016a), the presence of fractured parental material (as is the case in other Páramo catchments), $PasS_{(Q)}$ could be much higher than that estimated at the ZEO outlet (M7, 457 mm).

4.2. Dynamic water storage at the catchment scale

4.2.1. Long-term dynamic storage

The dynamics of the daily water storage volumes ($S(t)$) indicate a fast system response to precipitation inputs, with positive (i.e., recharge) and negative (i.e., discharge) values oscillating around a value of zero during the monitoring period (Fig. 2). Such system dynamics resulted in relatively low long-term $DynS$ ($DynS_{(LT)}$), with values ranging between 29 and 35 mm (Table 2) for all the catchments at the ZEO. These values were low compared with those reported by Peters and Aulenbach (2011) (40–70 mm), Buttle (2016) (30–77 mm), and Pfister et al. (2017) (107–373 mm) at other ecosystems with more drainable soils than those of the Páramo. On the other hand, Staudinger et al. (2017) found a wider range of values in Swiss pre-alpine and alpine catchments (12–974 mm), where catchments with similar values than the ZEO were rainfall-dominated and with only minor groundwater contributions. Soulsby et al. (2011) reported $DynS_{(LT)}$ values ranging between 2 and 36 mm in a group of montane Scottish catchments with similar pedological and land cover conditions to our sites. They concluded that values close to 36 mm corresponded to catchments with relatively compacted bedrock, whereas values close to 2 mm corresponded to catchments with high groundwater contributions (i.e., fractured parental material).

Long term dynamic storage at the ZEO was affected by the porosity and hydraulic conductivity contrast between the Histosols and the Andosols. Histosols presence was almost exclusively restricted to flat areas with low hydraulic gradients (i.e., valley bottoms and flat hill-tops). Consequently, their water movement was reduced and restricted mostly to the shallow rooted organic horizons (Correa et al., 2017; Mosquera et al., 2016a). In this sense, our relatively small $DynS_{(LT)}$ estimates, which likely result from the low available storage in the rooted zone of the organic horizon of the Histosol soils that are near saturation along the year (Mosquera et al., 2016a), suggest minimal unused storage during runoff generation. These findings are supported by our estimated $DynS_{(LT)}$ to $PasS_{(Q)}$ ratios for the ZEO catchments. These ratios also depicted that only a relatively small proportion of the water stored and available for mixing within the catchment is hydrologically active (i.e., 6 to 10% is active in the water balance, Table 2).

4.2.2. Event-based dynamic storage

The anticlockwise hysteretic-loop pattern between the normalized fractional storage (S_f) and the normalized fractional discharge (Q_f) (Fig. 3) identified at the event scale has also been determined by field observations elsewhere (e.g., Botter et al., 2009; Creutzfeldt et al., 2014; Beven and Davies, 2015; Hailegeorgis et al., 2016). Modelling studies have also shown this behavior (e.g., Kirchner, 2009; Davies and

Beven, 2015). The direction of the loop pattern has been shown to depend on different climatic, topographic, and parent material (Sproles et al., 2015). At the ZEO, the observed anticlockwise trend is likely explained by the combined effect of the Histosols (wetlands) high water retention capacity and the year-round input of low intensity precipitation. In other words, when water is added at the beginning of the event, it quickly fills the available storage before ‘effective precipitation’ drives the runoff that is released to the streams. Then, after antecedent moisture controlled storage threshold is reached (Mosquera et al., 2016a), the soils begin releasing water to streams (black lines in Fig. 3a and b). Once precipitation ceases, the moisture gained by the soils allows for a sustained stormflow generation until the end of the event (grey line in Fig. 3a and b), when the system returns to a stability condition (i.e., $S_f \approx 0$) because of the high water retention capacity of the soils. These findings further explain the rapid changes in daily $S(t)$ volumes (Fig. 2) and the flashy discharge response to precipitation previously reported at the ZEO (Mosquera et al., 2016b, 2015). Such behavior has also been reported by Fovet et al. (2015) in poorly drained riparian zones at a headwater catchment in France. The consistent anticlockwise direction observed during all monitored events at all catchments at ZEO further highlights the importance of the riparian Histosols in streamflow generation at the ZEO (Correa et al., 2017; Mosquera et al., 2016a).

4.2.3. How vegetation, soils, and precipitation control dynamic storage?

In the long term, the range of variation of $DynS_{(LT)}$ among catchments was very small (29–35 mm). As a result, we could not attribute their spatial variability to any particular catchment features or hydro-metric variables. On the other hand, at the event scale, $DynS_{(ES)}$ showed significant correlation with maximum P intensity (Fig. 5). This observation suggests that the amount of hydraulically active water linearly increases with rainfall intensity. This effect likely results from the rapid filling of unsaturated pores in the shallow (30–40 cm) organic horizon of the Páramo soils, which then augment the connectivity of saturated soil patches as precipitation intensity and amount increases (Tromp-van Meerveld and McDonnell, 2006; Tetzlaff et al., 2014). This effect causes a rapid activation of soil $DynS$, which in turn results in a rapid delivery of water towards the stream network during rainfall events.

4.3. A conceptual model of vegetation, soils, and precipitation controls on Páramo water storage

Our findings can be conceptualized in the context of the celerity of the hydraulic potentials (i.e., the propagation speed of a perturbation within the hydrologic system; McDonnell and Beven, 2014; Beven and Davies, 2015) in the Páramo soils and the tracer velocity through the hydrologic system. Combined hydrological behavior that influences the hydrological services provided by Páramo catchments. Fig. 6 shows how the rapid filling of available storage during rainfall events leads to rapid streamflow response (i.e., the system celerity response). This response behavior, in combination with low evapotranspiration due to the high year-round humidity (> 90%, Córdova et al., 2015), helps maintain the near saturated conditions of significant portions of the Páramo (i.e., the Histosol soils and wetlands). Thus, precipitation translates to runoff quickly via shallow subsurface flow in the first 30–40 cm of the Páramo soils (Mosquera et al., 2016a) and this in turn controls the water production capacity of Páramo catchments, as seen on the lefthand side of Fig. 6.

The righthand side of Fig. 6 depicts the attenuation of the stable isotopic composition in streamflow in relation to precipitation isotopic composition (Mosquera et al., 2016a) —which results from the relatively long time that water resides in the hydrologic system (Mosquera et al., 2016b). The relatively high $PasS$ values in the organic horizon of the soils at the ZEO shows that the velocity of the system is regulated by the high water retention capacity of the Páramo wetlands. This

retention capacity is maintained by the year-round input of low intensity precipitation (Padrón et al., 2015). This combination of factors control the water storage capacity, and thus, provide Páramo catchments with a high water regulation capacity (as shown on the righthand side of Fig. 6). As a result, when precipitation intensities increase, the system’s celerity perturbation is enhanced, and thus, a rapid response (minutes to hours) of $DynS$ occurs. This effect occurs despite the efficient mixing of tracer in the larger available $PasS$ of the wetlands soils (Mosquera et al., 2016a), which further reduces the velocity of the hydrologic system (weeks to months). This velocity reduction, in turn, increases the residence time of the isotopic tracer within the catchments. These findings highlight the vulnerability of Páramo catchments to changes in the temporal variability of precipitation and the potential changes in hydro-pedological conditions of the Páramo soils in response to changes in land use and climate.

For instance, this catchment hydrological behavior could be significantly altered by the impact of common anthropic practices in the study region. Previous studies have shown that pine afforestation decreased water yield and potato cultivation declined baseflow production in Páramo catchments (Buytaert et al., 2007). Similarly, afforestation with pine plantations has shown to decline significantly organic carbon and the water retention capacity of Páramo soils (Farley et al., 2004). These changes likely reflect a reduction in the MTT of water within the hydrologic system due to a significant reduction of the systems’ passive storage. Effect that is likely to result in a reduction of the flow regulation capacity of Páramo catchments.

Finally, it is worth highlighting the similarities of our catchment storage findings in comparison to those in other regions of the world (e.g., the Scottish highlands; Birkel et al., 2011; Soulsby et al., 2009; Tetzlaff et al., 2015a; van Huijgevoort et al., 2016), despite differences

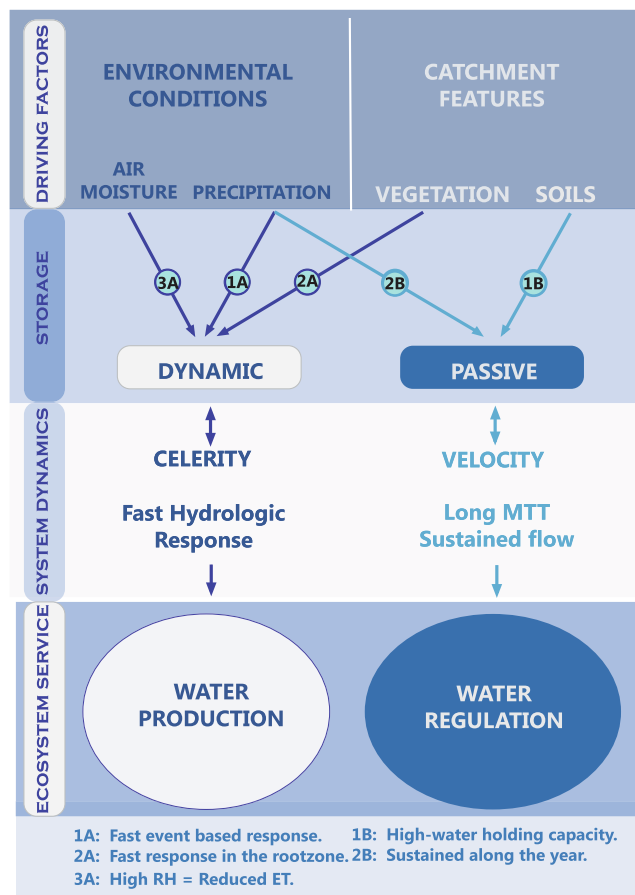


Fig. 6. Conceptual model of the factors influencing the Páramo water storage, hydrological dynamics, and ecosystem services provisioning.

in meteorological conditions. These similarities indicate that our findings can serve as a baseline for future water storage evaluations and could be transferable to other peat-dominated ecosystems in the Andes and elsewhere.

5. Conclusions

Our catchment storage evaluation using a combination of hydro-metric, isotopic, and hydrophysical soil properties data yielded valuable insights into the water passive and dynamic water storage of the Páramo. We demonstrated that streamflow mean transit time (MTT) is useful for estimating catchment passive storage (*PasS*) and these estimates are comparable with hydrophysical soil properties and soil water MTT based approaches. Together, these estimates provide a novel approach to infer groundwater contributions to catchment storage. We found that the hydrologically active dynamic storage (*DynS*) corresponded to only a small proportion (6–10%) of the total *PasS* capacity of the Andean Páramo wetlands that contribute to runoff generation. Our findings also indicate that the *DynS* and water production capacity of the catchments is mainly controlled by rainfall intensity. In contrast, *PasS* and water regulation capacity is controlled mostly by the high-water retention capacity of the peaty soils (Histosols). These findings provide baseline information about the factors controlling the water production and regulation ecosystem services provided by the Páramo. Future research should be targeted towards the investigation of the resilience of the Andean Páramo wetlands to sustain water production and regulation in response to changes in environmental conditions due to climate change and to better understand the role of hillslope soils (i.e., Andosols) in the provisioning of hydrological services in the Páramo and other high-elevation tropical environments.

Acknowledgments

This manuscript is an outcome of the MSc Program in Ecohydrology of the University of Cuenca. We would like to thank INV Metals S.A. (Loma Larga Project) for the assistance in the logistics during the study period. The authors also want to thank Irene Cardenas for her support with the laboratory analyses and Franklin Marin for his support with the collection of soil samples for hydrophysical properties analyses. G. M. M. also thanks the support of the University of Cuenca's Doctoral Program in Water Resources. We also thank Editor Marco Borgia, Conrado Tobón, and an anonymous reviewer for their valuable comments on earlier versions of this manuscript.

Funding

This research was funded by the Ecuadorian Secretary of Higher Education, Science, Technology and Innovation (SENESCYT) in the framework of the project “Desarrollo de indicadores hidrológicos funcionales para la evaluación del impacto del cambio global en ecosistemas Andinos”, and by the Central Research Office of the University of Cuenca (DIUC) in the framework of the project “Desarrollo de indicadores hidrológicos funcionales para evaluar la influencia de las laderas y humedales en una cuenca de Páramo Húmedo”.

Conflict of interest

The authors declare no conflict of interest.

References

Allen, R., Pereira, L., Raes, D., Smith, M., 1998. *Crop Evapotranspiration-Guidelines for Computing Crop Water Requirements-FAO Irrigation and Drainage Paper 56*. FAO, Rome.

Amvrosiadi, N., Seibert, J., Grabs, T., Bishop, K., 2017. Water storage dynamics in a till hillslope: the foundation for modeling flows and turnover times. *Hydrol. Process.* 31, 4–14. <https://doi.org/10.1002/hyp.11046>.

Aparecido, L.M.T., Teodoro, G.S., Mosquera, G., Brum, M., Barros, F. de V., Pompeu, P.V., Rodas, M., Lazo, P., Müller, C.S., Mulligan, M., Asbjornsen, H., Moore, G.W., Oliveira, R.S., 2018. Ecohydrological drivers of Neotropical vegetation in montane ecosystems. *Ecohydrology* e1932. <https://doi.org/10.1002/eco.1932>.

Asbjornsen, H., Manson, R.H., Scullion, J.J., Holwerda, F., Muñoz-Villers, L.E., Alvarado-Barrientos, M.S., Geissert, D., Dawson, T.E., McDonnell, J.J., Bruijnzeel, L.A., 2017. Interactions between payments for hydrologic services, landowner decisions, and ecohydrological consequences: synergies and disconnection in the cloud forest zone of central Veracruz, Mexico. *Ecol. Soc.* 22 <https://doi.org/10.5751/ES-09144-220225>. art25.

Beven, K., Davies, J., 2015. Velocities, celerities and the basin of attraction in catchment response. *Hydrol. Process.* 29, 5214–5226. <https://doi.org/10.1002/hyp.10699>.

Birkel, C., Soulsby, C., 2016. Linking tracers, water age and conceptual models to identify dominant runoff processes in a sparsely monitored humid tropical catchment. *Hydrol. Process.* 30, 4477–4493. <https://doi.org/10.1002/hyp.10941>.

Birkel, C., Soulsby, C., Tetzlaff, D., 2011. Modelling catchment-scale water storage dynamics: reconciling dynamic storage with tracer-inferred passive storage. *Hydrol. Process.* 25, 3924–3936. <https://doi.org/10.1002/hyp.8201>.

Bishop, K., Seibert, J., Nyberg, L., Rodhe, A., 2011. Water storage in a till catchment. II: Implications of transmissivity feedback for flow paths and turnover times. *Hydrol. Process.* 25, 3950–3959. <https://doi.org/10.1002/hyp.8355>.

Boll, J., Selker, J.S., Nijssen, B.M., Steenhuis, T.S., Van Winkle, J., Jolles, E., 1991. *Water quality sampling under preferential flow conditions*. In: Allen, R.G., Howell, T.A., Pruitt, W.O., Walter, I.A., Jensen, M.E. (Eds.), *Lysimeters for Evapotranspiration and Environmental Measurements*. American Society of Civil Engineers, New York, pp. 290–298.

Boll, J., Steenhuis, T.S., Selker, J.S., 1992. Fiberglass Wicks for Sampling of Water and Solutes in the Vadose Zone. *Soil Sci. Soc. Am. J.* 56, 701. <https://doi.org/10.2136/sssaj1992.03615995005600030005x>.

Botter, G., Porporato, A., Rodriguez-Iturbe, I., Rinaldo, A., 2009. Nonlinear storage-discharge relations and catchment streamflow regimes. *Water Resour. Res.* 45. <https://doi.org/10.1029/2008WR007658>.

Brauer, C.C., Teuling, A.J., Torfs, P.J.J.F., Uijlenhoet, R., 2013. Investigating storage-discharge relations in a lowland catchment using hydrograph fitting, recession analysis, and soil moisture data. *Water Resour. Res.* 49, 4257–4264. <https://doi.org/10.1002/wrcr.20320>.

Brauman, K.A., Daily, G.C., Duarte, T.K., Mooney, H.A., 2007. The nature and value of ecosystem services: an overview highlighting hydrologic services. *Annu. Rev. Environ. Resour.* 32, 67–98. <https://doi.org/10.1146/annurev.energy.32.031306.102758>.

Buttle, J.M., 2016. Dynamic storage: a potential metric of inter-basin differences in storage properties. *Hydrol. Process.* 30, 4644–4653. <https://doi.org/10.1002/hyp.10931>.

Buytaert, W., 2004. *The Properties of the Soils of the South Ecuadorian Páramo and the Impact of Land Use Changes on their Hydrology*. Katholieke Universiteit Leuven.

Buytaert, W., Beven, K., 2011. Models as multiple working hypotheses: hydrological simulation of tropical alpine wetlands. *Hydrol. Process.* 25, 1784–1799. <https://doi.org/10.1002/hyp.7936>.

Buytaert, W., Celleri, R., Willems, P., Bièvre, B. De, Wyseure, G., 2006. Spatial and temporal rainfall variability in mountainous areas: a case study from the south Ecuadorian Andes. *J. Hydrol.* 329, 413–421. <https://doi.org/10.1016/j.jhydrol.2006.02.031>.

Buytaert, W., Iniguez, V., Bièvre, B. De, 2007. The effects of afforestation and cultivation on water yield in the Andean páramo. *For. Ecol. Manage.* 251, 22–30. <https://doi.org/10.1016/j.foreco.2007.06.035>.

Coltorti, M., Ollier, C., 2000. Geomorphic and tectonic evolution of the Ecuadorian Andes. *Geomorphology* 32, 1–19. [https://doi.org/10.1016/S0169-555X\(99\)00036-7](https://doi.org/10.1016/S0169-555X(99)00036-7).

Córdova, M., Carrillo-Rojas, G., Crespo, P., Wilcox, B., Céleri, R., 2015. Evaluation of the Penman-Monteith (FAO 56 PM) method for calculating reference evapotranspiration using limited data. *Mt. Res. Dev.* 35, 230–239. <https://doi.org/10.1659/MRD-JOURNAL-D-14-0024.1>.

Córdova, M., Céleri, R., Shellito, C.J., Orellana-Alvear, J., Abril, A., Carrillo-Rojas, G., 2016. Near-surface air temperature lapse rate over complex terrain in the southern Ecuadorian andes: implications for temperature mapping. *Arctic Antarct. Alp. Res.* 48, 673–684. <https://doi.org/10.1657/AAAR0015-077>.

Correa, A., Windhorst, D., Crespo, P., Céleri, R., Feyen, J., Breuer, L., 2016. Continuous versus event-based sampling: how many samples are required for deriving general hydrological understanding on Ecuador's páramo region? *Hydrol. Process.* 30, 4059–4073. <https://doi.org/10.1002/hyp.10975>.

Correa, A., Windhorst, D., Tetzlaff, D., Crespo, P., Céleri, R., Feyen, J., Breuer, L., 2017. Temporal dynamics in dominant runoff sources and flow paths in the Andean Páramo. *Water Resour. Res.* 53, 5998–6017. <https://doi.org/10.1002/2016WR020187>.

Cowie, R.M., Knowles, J.F., Dailey, K.R., Williams, M.W., Mills, T.J., Molotch, N.P., 2017. Sources of streamflow along a headwater catchment elevational gradient. *J. Hydrol.* <https://doi.org/10.1016/j.jhydrol.2017.03.044>.

Craig, H., 1961. Standard for reporting concentrations of deuterium and oxygen-18 in natural waters. *Science* 133, 1833–1834. <https://doi.org/10.1126/science.133.3467.1833>.

Crespo, P., Bückler, A., Feyen, J., Vaché, K.B., Frede, H.-G., Breuer, L., 2012. Preliminary evaluation of the runoff processes in a remote montane cloud forest basin using mixing model analysis and mean transit time. *Hydrol. Process.* 26, 3896–3910. <https://doi.org/10.1002/hyp.8382>.

Crespo, P.J., Feyen, J., Buytaert, W., Bückler, A., Breuer, L., Frede, H.-G., Ramírez, M., 2011. Identifying controls of the rainfall-runoff response of small catchments in the tropical Andes (Ecuador). *J. Hydrol.* 407, 164–174. <https://doi.org/10.1016/j.jhydrol.2011.03.044>.

- [jhydrol.2011.07.021](https://doi.org/10.1016/j.jhydrol.2011.07.021).
- Creutzfeldt, B., Troch, P.A., Güntner, A., Ferré, T.P.A., Graeff, T., Merz, B., 2014. Storage-discharge relationships at different catchment scales based on local high-precision gravimetry. *Hydrol. Process.* 28, 1465–1475. <https://doi.org/10.1002/hyp.9689>.
- Davies, J.A.C., Beven, K., 2015. Hysteresis and scale in catchment storage, flow and transport. *Hydrol. Process.* 29, 3604–3615. <https://doi.org/10.1002/hyp.10511>.
- Detty, J.M., McGuire, K.J., 2010. Threshold changes in storm runoff generation at a till-manifested headwater catchment. *Water Resour. Res.* 46. <https://doi.org/10.1029/2009WR008102>.
- Dunkerley, D., 2008. Identifying individual rain events from pluviograph records: a review with analysis of data from an Australian dryland site. *Hydrol. Process.* 22, 5024–5036. <https://doi.org/10.1002/hyp.7122>.
- Dunn, S.M., Birkel, C., Tetzlaff, D., Soulsby, C., 2010. Transit time distributions of a conceptual model: their characteristics and sensitivities. *Hydrol. Process.* 24, 1719–1729. <https://doi.org/10.1002/hyp.7560>.
- FAO, 2009. Guidelines for Soil Description. Food and Agriculture Organization of the United Nations.
- Farley, K.A., Kelly, E.F., Hofstede, R.G.M., 2004. Soil organic carbon and water retention after conversion of grasslands to pine plantations in the Ecuadorian Andes. *Ecosystems* 7, 729–739. <https://doi.org/10.1007/s10021-004-0047-5>.
- Fischer, B.M.C., van Meerveld, H.J. (Ilja), Seibert, J., 2017. Spatial variability in the isotopic composition of rainfall in a small headwater catchment and its effect on hydrograph separation. *J. Hydrol.* 547, 755–769. <https://doi.org/10.1016/j.jhydrol.2017.01.045>.
- Fovet, O., Ruiz, L., Hrachowitz, M., Fauchoux, M., Gascuel-Odoux, C., 2015. Hydrological hysteresis and its value for assessing process consistency in catchment conceptual models. *Hydrol. Earth Syst. Sci.* 19, 105–123. <https://doi.org/10.5194/hess-19-105-2015>.
- Geris, J., Tetzlaff, D., McDonnell, J., Soulsby, C., 2015a. The relative role of soil type and tree cover on water storage and transmission in northern headwater catchments. *Hydrol. Process.* 29, 1844–1860. <https://doi.org/10.1002/hyp.10289>.
- Geris, J., Tetzlaff, D., McDonnell, J.J., Soulsby, C., 2017. Spatial and temporal patterns of soil water storage and vegetation water use in humid northern catchments. *Sci. Total Environ.* 595, 486–493. <https://doi.org/10.1016/j.scitotenv.2017.03.275>.
- Geris, J., Tetzlaff, D., Soulsby, C., 2015b. Resistance and resilience to droughts: hydro-pedological controls on catchment storage and run-off response. *Hydrol. Process.* 29, 4579–4593. <https://doi.org/10.1002/hyp.10480>.
- Grant, L., Seyfried, M., McNamara, J., 2004. Spatial variation and temporal stability of soil water in a snow-dominated, mountain catchment. *Hydrol. Process.* 18, 3493–3511. <https://doi.org/10.1002/hyp.5798>.
- Guio Blanco, C.M., Brito Gomez, V.M., Crespo, P., Lief, M., 2018. Spatial prediction of soil water retention in a Páramo landscape: methodological insight into machine learning using random forest. *Geoderma* 316, 100–114. <https://doi.org/10.1016/j.geoderma.2017.12.002>.
- Hailegeorgis, T.T., Alfredsen, K., Abdella, Y.S., Kolberg, S., 2016. Evaluation of storage–discharge relationships and recession analysis-based distributed hourly runoff simulation in large-scale, mountainous and snow-influenced catchment. *Hydrol. Sci. J.* 61, 2872–2886. <https://doi.org/10.1080/02626667.2016.1170939>.
- Hale, V.C., McDonnell, J.J., Stewart, M.K., Solomon, D.K., Doolittle, J., Ice, G.G., Pack, R.T., 2016. Effect of bedrock permeability on stream base flow mean transit time scaling relationships: 2. Process study of storage and release. *Water Resour. Res.* 52, 1375–1397. <https://doi.org/10.1002/2015WR017660>.
- Hamel, P., Riveros-Iregui, D., Ballari, D., Browning, T., Céleri, R., Chandler, D., Chun, K.P., Destouni, G., Jacobs, S., Jasechko, S., Johnson, M., Krishnaswamy, J., Poca, M., Pompeu, P.V., Rocha, H., 2017. Watershed services in the humid tropics: opportunities from recent advances in ecohydrology. *Ecohydrology*. <https://doi.org/10.1002/eco.1921>. e1921.
- Hasan, S., Troch, P.A., Bogaart, P.W., Kroner, C., 2008. Evaluating catchment-scale hydrological modeling by means of terrestrial gravity observations. *Water Resour. Res.* 44. <https://doi.org/10.1029/2007WR006321>.
- Heidbüchel, I., Güntner, A., Blume, T., 2015. Use of cosmic ray neutron sensors for soil moisture monitoring in forests. *Hydrol. Earth Syst. Sci. Discuss.* 12, 9813–9864. <https://doi.org/10.5194/hessd-12-9813-2015>.
- Hofstede, R.G.M., Mena, V., Segarra, P., 2003. Los Paramos del Mundo.
- Holder, M.W., Brown, K.W., Thomas, J.C., Development of A Capillary Wick Unsaturated Zone Pore Water Sampler, U.S. Environmental Protection Agency, Washington, D.C., 1989. Development of a Capillary Wick Unsaturated Zone Pore Water Sampler. Environmental Monitoring Systems Laboratory, Office of Research and Development, United States Environmental Protection Agency.
- IAEA, 1997. Technical Procedure for Cumulative Monthly Sampling of Precipitation for Isotopic Analyses.
- IUCN, 2002. High Andean Wetlands. Gland, Switzerland.
- IUSS Working Group WRB, 2015. World Reference Base for Soil Resources 2014, update 2015. International soil classification system for naming soils and creating legends for soil maps. World Soil Resources Reports No. 106. FAO Rome.
- Kirchner, J.W., 2009. Catchments as simple dynamical systems: catchment characterization, rainfall-runoff modeling, and doing hydrology backward. *Water Resour. Res.* 45, 1–34. <https://doi.org/10.1029/2008WR006912>.
- Kirchner, J.W., Feng, X., Neal, C., 2000. Fractal stream chemistry and its implications for contaminant transport in catchments. *Nature* 403, 524–527. <https://doi.org/10.1038/35000537>.
- Knutson, J.H., Lee, S.B., Zhang, W.Q., Selker, J.S., 1993. Fiberglass wick preparation for use in passive capillary wick soil pore-water samplers. *Soil Sci. Soc. Am. J.* 57, 1474. <https://doi.org/10.2136/sssaj1993.03615995005700060013x>.
- Landon, M., Delin, G., Komor, S., Regan, C., 1999. Comparison of the stable-isotopic composition of soil water collected from suction lysimeters, wick samplers, and cores in a sandy unsaturated zone. *J. Hydrol.* 224, 45–54. [https://doi.org/10.1016/S0022-1694\(99\)00120-1](https://doi.org/10.1016/S0022-1694(99)00120-1).
- Lehmann, P., Hinz, C., McGrath, G., Tromp-van Meerveld, H.J., McDonnell, J.J., 2007. Rainfall threshold for hillslope outflow: an emergent property of flow pathway connectivity. *Hydrol. Earth Syst. Sci.* 11, 1047–1063. <https://doi.org/10.5194/hess-11-1047-2007>.
- Maloszewski, P., Zuber, A., 1996. Lumped parameter models for the interpretation of environmental tracer data. In: *Manual on Mathematical Models in Isotope Hydrogeology*. TECDOC-910.
- Maloszewski, P., Zuber, A., 1982. Determining the turnover time of groundwater systems with the aid of environmental tracers. *J. Hydrol.* 57, 207–231. [https://doi.org/10.1016/0022-1694\(82\)90147-0](https://doi.org/10.1016/0022-1694(82)90147-0).
- McDonnell, J.J., Beven, K., 2014. Debates-The future of hydrological sciences: a (common) path forward? a call to action aimed at understanding velocities, celerities and residence time distributions of the headwater hydrograph. *Water Resour. Res.* 50, 5342–5350. <https://doi.org/10.1002/2013WR015141>.
- McGuire, K.J., McDonnell, J.J., 2006. A review and evaluation of catchment transit time modeling. *J. Hydrol.* 330, 543–563. <https://doi.org/10.1016/j.jhydrol.2006.04.020>.
- McGuire, K.J., McDonnell, J.J., Weiler, M., Kendall, C., McGlynn, B.L., Welker, J.M., Seibert, J., 2005. The role of topography on catchment-scale water residence time. *Water Resour. Res.* 41, n/a-n/a. <https://doi.org/10.1029/2004WR003657>.
- Mcnamara, J.P., Tetzlaff, D., Bishop, K., Soulsby, C., Seyfried, M., Peters, N.E., Aulenbach, B.T., Hooper, R., 2011. Storage as a metric of catchment comparison. *Hydrol. Process.* 25, 3364–3371. <https://doi.org/10.1002/hyp.8113>.
- Moore, R.B., 2004. Introduction to salt dilution gauging for streamflow measurement Part 2: constant-rate injection. *Streamline Watershed Manag. Bull.* 8, 11–15.
- Mosquera, G.M., Céleri, R., Lazo, P.X., Vaché, K.B., Perakis, S.S., Crespo, P., 2016a. Combined use of isotopic and hydrometric data to conceptualize ecohydrological processes in a high-elevation tropical ecosystem. *Hydrol. Process.* 30, 2930–2947. <https://doi.org/10.1002/hyp.10927>.
- Mosquera, G.M., Lazo, P.X., Céleri, R., Wilcox, B.P., Crespo, P., 2015. Runoff from tropical alpine grasslands increases with areal extent of wetlands. *CATENA* 125, 120–128. <https://doi.org/10.1016/j.catena.2014.10.010>.
- Mosquera, G.M., Segura, C., Vaché, K.B., Windhorst, D., Breuer, L., Crespo, P., 2016b. Insights into the water mean transit time in a high-elevation tropical ecosystem. *Hydrol. Earth Syst. Sci.* 20, 2987–3004. <https://doi.org/10.5194/hess-20-2987-2016>.
- Nippen, F., McGlynn, B.L., Emanuel, R.E., 2015. The spatial and temporal evolution of contributing areas. *Water Resour. Res.* 51, 4550–4573. <https://doi.org/10.1002/2014WR016719>.
- Padrón, R.S., Wilcox, B.P., Crespo, P., Céleri, R., 2015. Rainfall in the Andean Páramo: new insights from high-resolution monitoring in Southern Ecuador. *J. Hydrometeorol.* 16, 985–996. <https://doi.org/10.1175/JHM-D-14-0135.1>.
- Pearce, A.J., Stewart, M.K., Sklash, M.G., 1986. Storm runoff generation in humid headwater catchments: 1. Where does the water come from? *Water Resour. Res.* 22, 1263–1272. <https://doi.org/10.1029/WR022i008p01263>.
- Penna, D., Stenni, B., Šanda, M., Wrede, S., Bogaard, T.A., Michelini, M., Fischer, B.M.C., Gobbi, A., Mantese, N., Zuecco, G., Borga, M., Bonazza, M., Sobotková, M., Čejková, B., Wassenaar, L.L., 2012. Technical note: evaluation of between-sample memory effects in the analysis of $\delta^2\text{H}$ and $\delta^{18}\text{O}$ of water samples measured by laser spectrometers. *Hydrol. Earth Syst. Sci.* 16, 3925–3933. <https://doi.org/10.5194/hess-16-3925-2012>.
- Peters, N.E., Aulenbach, B.T., 2011. Water storage at the Panola Mountain Research Watershed, Georgia, USA. *Hydrol. Process.* 25, 3878–3889. <https://doi.org/10.1002/hyp.8334>.
- Pfister, L., Martínez-Carreras, N., Hissler, C., Klaus, J., Carrer, G.E., Stewart, M.K., McDonnell, J.J., 2017. Bedrock geology controls on catchment storage, mixing, and release: a comparative analysis of 16 nested catchments. *Hydrol. Process.* 31, 1828–1845. <https://doi.org/10.1002/hyp.11134>.
- Picarro, 2010. ChemCorrect TM-Solving the Problem of Chemical Contaminants in H2O Stable Isotope Research, PICARRO INC, California, USA.
- Polk, M.H., Young, K.R., Baraer, M., Mark, B.G., McKenzie, J.M., Bury, J., Carey, M., 2017. Exploring hydrologic connections between tropical mountain wetlands and glacier recession in Peru's Cordillera Blanca. *Appl. Geogr.* 78, 94–103. <https://doi.org/10.1016/j.apgeog.2016.11.004>.
- Poulenard, J., Podwojewski, P., Herbillon, A.J., 2003. Characteristics of non-allophanic Andisols with hydric properties from the Ecuadorian páramos. *Geoderma* 117, 267–281. [https://doi.org/10.1016/S0016-7061\(03\)00128-9](https://doi.org/10.1016/S0016-7061(03)00128-9).
- Quichimbo, P., Tenorio, G., Borja, P., Cárdenas, I., Crespo, P., Céleri, R., 2012. Efectos sobre las propiedades físicas y químicas de los suelos por el cambio de la cobertura vegetal y uso del suelo: Páramo de Quimsacocha al sur del Ecuador. *Suelos Ecuatoriales* 42, 138–153.
- Roa-García, M.C., Weiler, M., 2010. Integrated response and transit time distributions of watersheds by combining hydrograph separation and long-term transit time modeling. *Hydrol. Earth Syst. Sci.* 14, 1537–1549. <https://doi.org/10.5194/hess-14-1537-2010>.
- Rosenberg, E.A., Clark, E.A., Steinemann, A.C., Lettenmaier, D.P., 2012. On the contribution of groundwater storage to interannual streamflow anomalies in the Colorado River basin. *Hydrol. Earth Syst. Sci. Discuss.* 9, 13191–13230. <https://doi.org/10.5194/hessd-9-13191-2012>.
- Safeeq, M., Hunsaker, C.T., 2016. Characterizing runoff and water yield for headwater catchments in the Southern Sierra Nevada. *JAWRA J. Am. Water Resour. Assoc.* 52, 1327–1346. <https://doi.org/10.1111/1752-1688.12457>.
- Sayama, T., McDonnell, J.J., 2009. A new time-space accounting scheme to predict stream water residence time and hydrograph source components at the watershed scale. *Water Resour. Res.* 45, W07401. <https://doi.org/10.1029/2008WR007549>.
- Sayama, T., McDonnell, J.J., Dhakal, A., Sullivan, K., 2011. How much water can a

- watershed store? *Hydrol. Process.* 25, 3899–3908. <https://doi.org/10.1002/hyp.8288>.
- Schoeneberger, P.J., Wysocki, D.A., Benham, E.C., Staff, S.S., 2012. *Field Book for Describing and Sampling Soils, Version 3.0*. National Soil Survey Center, Lincoln, NE.
- Seminario, S., 2016. Incertidumbre en la Precipitación Espacial Diaria Causada por redes Pluviográficas Dispersas en una Microcuenca de Páramo densamente Monitoreada. Universidad de Cuenca.
- Seyfried, M.S., Grant, L.E., Marks, D., Winstral, A., McNamara, J., 2009. Simulated soil water storage effects on streamflow generation in a mountainous snowmelt environment, Idaho, USA. *Hydrol. Process.* 23, 858–873. <https://doi.org/10.1002/hyp.7211>.
- Sidle, R.C., Noguchi, S., Tsuboyama, Y., Laursen, K., 2001. A conceptual model of preferential flow systems in forested hillslopes: evidence of self-organization. *Hydrol. Process.* 15, 1675–1692. <https://doi.org/10.1002/hyp.233>.
- Sidle, R.C., Tsuboyama, Y., Noguchi, S., Hosoda, I., Fujieda, M., Shimizu, T., 1995. Seasonal hydrologic response at various spatial scales in a small forested catchment, Hitachi Ohta. Japan. *J. Hydrol.* 168, 227–250. [https://doi.org/10.1016/0022-1694\(94\)02639-S](https://doi.org/10.1016/0022-1694(94)02639-S).
- Smakhtin, V., 2001. Low flow hydrology: a review. *J. Hydrol.* 240, 147–186. [https://doi.org/10.1016/S0022-1694\(00\)00340-1](https://doi.org/10.1016/S0022-1694(00)00340-1).
- Soulsby, C., Birkel, C., Geris, J., Dick, J., Tunaley, C., Tetzlaff, D., 2015. Stream water age distributions controlled by storage dynamics and nonlinear hydrologic connectivity: modeling with high-resolution isotope data. *Water Resour. Res.* 51, 7759–7776. <https://doi.org/10.1002/2015WR017888>.
- Soulsby, C., Birkel, C., Tetzlaff, D., 2016. Modelling storage-driven connectivity between landscapes and riverscapes: towards a simple framework for long-term ecohydrological assessment. *Hydrol. Process.* 30, 2482–2497. <https://doi.org/10.1002/hyp.10862>.
- Soulsby, C., Neal, C., Laudon, H., Burns, D.A., Merot, P., Bonell, M., Dunn, S.M., Tetzlaff, D., 2008. Catchment data for process conceptualization: simply not enough? *Hydrol. Process.* 22, 2057–2061. <https://doi.org/10.1002/hyp.7068>.
- Soulsby, C., Piegat, K., Seibert, J., Tetzlaff, D., 2011. Catchment-scale estimates of flow path partitioning and water storage based on transit time and runoff modelling. *Hydrol. Process.* 25, 3960–3976. <https://doi.org/10.1002/hyp.8324>.
- Soulsby, C., Tetzlaff, D., 2008. Towards simple approaches for mean residence time estimation in ungauged basins using tracers and soil distributions. *J. Hydrol.* 363, 60–74. <https://doi.org/10.1016/j.jhydrol.2008.10.001>.
- Soulsby, C., Tetzlaff, D., Hrachowitz, M., 2009. Tracers and transit times: windows for viewing catchment scale storage? *Hydrol. Process.* 23, 3503–3507. <https://doi.org/10.1002/hyp.7501>.
- Spence, C., 2007. On the relation between dynamic storage and runoff: a discussion on thresholds, efficiency, and function. *Water Resour. Res.* 43, n/a–n/a. <https://doi.org/10.1029/2006WR005645>.
- Spence, C., Guan, X.J., Phillips, R., 2011. The Hydrological Functions of a Boreal Wetland. *Wetlands* 31, 75–85. <https://doi.org/10.1007/s13157-010-0123-x>.
- Sproles, E.A., Leibowitz, S.G., Reager, J.T., Wigington, P.J., Famiglietti, J.S., Patil, S.D., 2015. GRACE storage-runoff hystereses reveal the dynamics of regional watersheds. *Hydrol. Earth Syst. Sci.* 19, 3253–3272. <https://doi.org/10.5194/hess-19-3253-2015>.
- Staudinger, M., Stoelzle, M., Seeger, S., Seibert, J., Weiler, M., Stahl, K., 2017. Catchment water storage variation with elevation. *Hydrol. Process.* 31, 2000–2015. <https://doi.org/10.1002/hyp.11158>.
- Sucozhañay, A., Célteri, R., 2018. Impact of rain gauges distribution on the runoff simulation of a small mountain catchment in Southern Ecuador. *Water* 10, 1169. <https://doi.org/10.3390/w10091169>.
- Sun, G., Hallema, D., Asbjornsen, H., 2017. Ecohydrological processes and ecosystem services in the Anthropocene: a review. *Ecol. Process.* 6, 35. <https://doi.org/10.1186/s13717-017-0104-6>.
- Tetzlaff, D., Birkel, C., Dick, J., Geris, J., Soulsby, C., 2014. Storage dynamics in hydro-pedological units control hillslope connectivity, runoff generation, and the evolution of catchment transit time distributions. *Water Resour. Res.* 50, 969–985. <https://doi.org/10.1002/2013WR014147>.
- Tetzlaff, D., Buttle, J., Carey, S.K., McGuire, K., Laudon, H., Soulsby, C., 2015a. Tracer-based assessment of flow paths, storage and runoff generation in northern catchments: a review. *Hydrol. Process.* 29, 3475–3490. <https://doi.org/10.1002/hyp.10412>.
- Tetzlaff, D., Buttle, J., Carey, S.K., van Huijgevoort, M.H.J., Laudon, H., McNamara, J.P., Mitchell, C.P.J., Spence, C., Gabor, R.S., Soulsby, C., 2015b. A preliminary assessment of water partitioning and ecohydrological coupling in northern headwaters using stable isotopes and conceptual runoff models. *Hydrol. Process.* 29, 5153–5173. <https://doi.org/10.1002/hyp.10515>.
- Tromp-van Meerveld, H.J., McDonnell, J.J., 2006. Threshold relations in subsurface stormflow: 2. The fill and spill hypothesis. *Water Resour. Res.* 42. <https://doi.org/10.1029/2004WR003800>.
- U.S. Bureau of Reclamation, 2001. *Water Measurement Manual*. Washington DC.
- USDA, NRCS, 2004. *Soil Survey Laboratory Methods Manual: Soil Survey Investigations Report No. 42, Version 4.0, November 2004*. United States Department of Agriculture Natural Resources Conservation Service.
- van Huijgevoort, M.H.J., Tetzlaff, D., Sutanudjaja, E.H., Soulsby, C., 2016. Using high resolution tracer data to constrain water storage, flux and age estimates in a spatially distributed rainfall-runoff model. *Hydrol. Process.* 30, 4761–4778. <https://doi.org/10.1002/hyp.10902>.
- Viviroli, D., Dürr, H.H., Messerli, B., Meybeck, M., Weingartner, R., 2007. Mountains of the world, water towers for humanity: typology, mapping, and global significance. *Water Resour. Res.* 43. <https://doi.org/10.1029/2006WR005653>.
- Weiler, M., McGlynn, B.L., McGuire, K.J., McDonnell, J.J., 2003. How does rainfall become runoff? a combined tracer and runoff transfer function approach. *Water Resour. Res.* 39, n/a–n/a. <https://doi.org/10.1029/2003WR002331>.
- Wright, C., Kagawa-Viviani, A., Gerlein-Safdi, C., Mosquera, G.M., Poca, M., Tseng, H., Chun, K.P., 2017. Advancing ecohydrology in the changing tropics: perspectives from early career scientists. *Ecohydrology* e1918. <https://doi.org/10.1002/eco.1918>.